© 2020. Published by The Company of Biologists Ltd | Journal of Cell Science (2020) 133, jcs246199. doi:10.1242/jcs.246199

RESEARCH ARTICLE

Integration of JAK/STAT receptor–ligand trafficking, signalling and gene expression in *Drosophila melanogaster* cells

Rachel Moore[1], Katja Vogt[1,*], Adelina E. Acosta-Martin[2], Patrick Shire[1], Martin Zeidler[1] and Elizabeth Smythe[1,‡]

ABSTRACT

The JAK/STAT pathway is an essential signalling cascade required for multiple processes during development and for adult homeostasis. A key question in understanding this pathway is how it is regulated in different cell contexts. Here, we have examined how endocytic processing contributes to signalling by the single cytokine receptor in *Drosophila melanogaster* cells, Domeless. We identify an evolutionarily conserved di-leucine (di-Leu) motif that is required for Domeless internalisation and show that endocytosis is required for activation of a subset of Domeless targets. Our data indicate that endocytosis both qualitatively and quantitatively regulates Domeless signalling. STAT92E, the single STAT transcription factor in *Drosophila*, appears to be the target of endocytic regulation, and our studies show that phosphorylation of STAT92E on Tyr704, although necessary, is not always sufficient for target transcription. Finally, we identify a conserved residue, Thr702, which is essential for Tyr704 phosphorylation. Taken together, our findings identify previously unknown aspects of JAK/STAT pathway regulation likely to play key roles in the spatial and temporal regulation of signalling *in vivo*.

KEY WORDS: *Drosophila*, JAK/STAT, Endocytosis, Signalling

INTRODUCTION

The Janus kinase/signal transducer and activator of transcription (JAK/STAT) signalling pathway regulates a variety of cellular events, including proliferation and apoptosis, throughout development and in adult life (Villarino et al., 2017). According to the canonical model, JAK/STAT signalling involves the activation of homo- or hetero-dimerised cell-surface transmembrane receptors by ligands, including cytokines, growth factors and hormones, which causes a conformational change in the cytoplasmic tail of the receptor. This stimulates activation of the Janus kinases (JAKs) that are constitutively associated with the receptor. JAK activation leads to specific Tyr phosphorylation of both the kinase and the receptor, subsequently allowing recruitment of signal transducer and activator of transcription (STAT) transcription factors through Src-homology 2 (SH2) domains. This association in turn allows JAK to phosphorylate STATs at a highly conserved C-terminal Tyr residue, leading to STAT dimerisation and translocation to the nucleus. In the nucleus, STATs bind to palindromic DNA sequences to alter expression of target genes, resulting in developmental, haematological and immune-related responses (O'Shea et al., 2015; Stark and Darnell, 2012). Dysregulation of the JAK/STAT pathway is involved in the pathogenesis of diseases such as gigantism, asthma, myocardial hypertrophy, myeloproliferative neoplasia and severe combined immunodeficiency (O'Shea et al., 2015).

The JAK/STAT pathway has been highly conserved throughout evolution, with invertebrates such as *Drosophila melanogaster* having a full complement of pathway components. However, whereas mammals have multiple copies of receptors, JAKs and STATs, in *Drosophila* the signalling pathway is composed of a single positively acting receptor, Domeless (Dome) (Brown et al., 2001); a negatively acting receptor, Latran (also known as eye transformer, et; Makki et al., 2010); one JAK, Hopscotch (Hop); and one STAT, STAT92E (Hou et al., 1996; Yan et al., 1996; Zeidler and Bausek, 2013). Therefore, *Drosophila* provides an excellent model in which to investigate JAK/STAT pathway regulation, without the difficulties of compensation and signalling crosstalk inherent in mammalian systems. In fact, investigating JAK/STAT signalling in *Drosophila* has led to key breakthroughs in understanding the impact of its dysregulation in human disease (Ekas et al., 2010).

The repeated use of the JAK/STAT pathway in a variety of contexts begs the question as to how transcriptional outputs are differentially regulated in a cell- and tissue-specific manner. One potential mechanism to explain this diversity of outputs is regulation by endocytosis (Sigismund and Scita, 2018; Villaseñor et al., 2016; Weinberg and Puthenveedu, 2019). Activated receptors can be internalised into cells by multiple endocytic pathways, of which clathrin-mediated endocytosis (CME) is the best characterised. Receptor complexes internalised by CME are clustered into clathrin-coated pits. The assembled clathrin lattice is linked to the cytoplasmic domains of transmembrane receptors via adaptor proteins, including the AP2 adaptor complex (Mettlen et al., 2018; Owen et al., 2004). In addition to CME, several clathrin-independent (CIE) pathways exist, which are important for the uptake of particular cargoes (Mayor et al., 2014). Following internalisation, activated receptors are delivered to the early endosome where they may be recycled or targeted to late endosomes and lysosomes for degradation. The endosomal sorting complexes required for transport (ESCRT) protein complexes are key for sorting receptors into late endosomes and lysosomes. Hrs is a component of ESCRT-0, acting as an adaptor to select ubiquitylated cargo for targeting to lysosomes. TSG101 is a component of ESCRT-I complexes, which recruit other ESCRT complexes – a process key to allowing the inward invaginations of the late endosome to form intraluminal vesicles (Henne et al., 2013).

[1]Centre for Membrane Interactions and Dynamics, Department of Biomedical Science, University of Sheffield, Sheffield S10 2TN, UK. [2]biOMICS Facility, Faculty of Science Mass Spectrometry Centre, University of Sheffield, Sheffield S10 2TN, UK.
*Present address: School of Medicine, University of Central Lancaster, Preston PR1 2HE, UK.

‡Author for correspondence (e.smythe@sheffield.ac.uk)

M.Z., 0000-0003-2942-1135; E.S., 0000-0002-1430-5898

Handling Editor: Caroline Hill
Received 17 March 2020; Accepted 2 September 2020

Journal of Cell Science (2020) 133, jcs246199. doi:10.1242/jcs.246199

Results from *in vivo* and *in vitro* experiments indicate that endocytosis can regulate receptor signalling quantitatively through removal of activated receptors from the cell surface and targeting them to lysosomes for degradation. Endocytosis can also qualitatively regulate signalling by establishing 'signalosomes', which are membrane microdomains within endosomal compartments that allow the recruitment of specific scaffolds, adaptors, kinases and phosphatases, thus resulting in different downstream signalling outputs (Carroll and Dunlop, 2017; Lawrence et al., 2019; Moore et al., 2018; Sigismund and Scita, 2018; Villaseñor et al., 2016). The route of entry of activated receptors (CME versus CIE) can also influence signalling output, as demonstrated for Notch signalling in *Drosophila* (Shimizu et al., 2014) and TGF-β signalling in mammalian cells (Di Guglielmo et al., 2003). CME is a major entry portal that has been shown to regulate JAK/STAT signalling following activation of several different cytokine receptors in mammalian cells (Cendrowski et al., 2016; Chmiest et al., 2016; German et al., 2011; Kermorgant and Parker, 2008; Marchetti et al., 2006).

In vivo studies in *Drosophila* suggest that Dome-dependent border cell migration requires ligand-dependent CME and delivery to multivesicular bodies (Devergne et al., 2007). Mutation of endocytic components, including clathrin heavy chain (CHC), prevents Dome internalisation and decreases STAT92E expression and nuclear translocation in follicle cells. In contrast, endocytosis appears to negatively regulate JAK/STAT signalling in *Drosophila* Kc_{167} cells (Müller et al., 2008; Vidal et al., 2010). These varying results likely reflect differences due to cell context, as has been observed for endocytic regulation of receptor tyrosine kinases such as epidermal growth factor receptor (EGFR) (Sousa et al., 2012; Vieira et al., 1996; Villaseñor et al., 2015). The underlying regulatory mechanisms of context-dependent signalling are, however, largely unknown.

Canonical signalling by STAT requires phosphorylation at a conserved tyrosine residue (Tyr704 in *Drosophila* STAT92E, isoform C used in this study), which allows for parallel dimerisation of STATs via their SH2 domains and translocation into the nucleus. There is also evidence that other posttranslational modifications, in addition to phosphorylation of the conserved Tyr, regulate STAT activity (Chung et al., 1997; Costa-Pereira et al., 2011; Grönholm et al., 2010; Karsten et al., 2006; Wang et al., 2005).

Here, we show that in *Drosophila* S2R+ cells, endocytosis is essential for the expression of some, but not all, JAK/STAT pathway target genes. We demonstrate that STAT92E is the target for endocytic regulation and, importantly, that endocytosis qualitatively regulates STAT92E activity. In addition, we have identified a novel phosphorylation site, Thr702, which is crucial for phosphorylation of STAT92E on Tyr704.

RESULTS

Dome internalisation requires an evolutionarily conserved di-leucine cassette

To understand mechanisms of Dome internalisation, we first asked how Dome and its ligand Upd2 are taken into cells. Similar to mammalian cells, *Drosophila* cells can internalise material by a variety of CME and CIE mechanisms (Shimizu et al., 2014). It has been shown that Dome is internalised into *Drosophila* Kc_{167} cells by CME (Müller et al., 2008; Vidal et al., 2010). To investigate whether this is the case in S2R+ cells, we measured internalisation of Upd2–GFP, as a proxy for receptor internalisation, using an anti-GFP ELISA assay (Wright et al., 2011). We first treated cells with dsRNA targeting Dome and found that there is a significant reduction in the rate (−38%) and extent (−50%) of uptake of Upd2–GFP at both high (20 nM; Fig. 1A) and low (3 nM; Fig. S1A) concentrations of Upd2–GFP. Under these conditions, levels of Dome mRNA are reduced by ∼90% (Fig. S1B). The residual uptake of Upd2–GFP in the absence of Dome is likely due to non-specific fluid-phase uptake of ligand. When cells were incubated with 20 nM Upd2–GFP, knockdown of CHC and AP2 reduced the uptake of Upd2–GFP by ∼60% compared to knockdown of Dome alone (Fig. 1A). Because levels of CHC and AP2 mRNA were reduced by ∼80% following dsRNA knockdown (Fig. S1B and data not shown), this suggests that the Upd2–GFP complex can be internalised by CIE as well as CME, as has been shown for several receptors in mammalian cells (Sigismund et al., 2005; Vander Ark et al., 2018) and for Notch and Delta in *Drosophila* (Shimizu et al., 2014). By contrast, when S2R+ cells were incubated with low concentrations of Upd2–GFP (3 nM), knockdown of CHC reduced the uptake of Upd2–GFP to the level observed following Dome knockdown (Fig. S1A). Taken together this suggests that at low concentrations of Upd2–GFP, Dome is primarily internalised by CME, but that increasing concentrations of ligand results in Dome also being internalised via CIE.

Sorting of cargo into clathrin-coated pits requires internalisation motifs in the cytoplasmic tails of receptors that include both Tyr- and di-leucine (di-Leu)-based motifs (Traub, 2003). Dome is most similar in sequence and structure to gp130 (also known as IL6ST) of vertebrates, which is a co-receptor shared by receptors for IL-6 (Fig. 1B). Internalisation of gp130 requires a di-Leu motif (^{786}LL^{787}) in its cytoplasmic domain (Dittrich et al., 1996) while an upstream serine within the sequence ^{780}**S**ESTQP**LL**^{787} has also been shown to be important for rapid internalisation (Dittrich et al., 1996). Strikingly, the cytoplasmic tail of Dome also contains a di-Leu motif, ^{985}LL^{986}, in a similar context to that of the di-Leu motif in gp130 (Fig. 1C). In order to test the potential significance of this motif, we generated a series of FLAG-tagged Dome mutant constructs where individual elements of the di-Leu cassette were mutated either alone or in combination (Fig. 1C), and transfected these constructs into S2R+ cells. To quantitatively measure ligand-dependent uptake of the engineered Dome constructs, proteins on the surface of transfected S2R+ cells were biotinylated prior to addition of Upd2–GFP. This showed that, although expression of the mutants was somewhat more efficient than that following transfection of wild-type Dome (Fig. S1C), plasma membrane expression of all the constructs was comparable (Fig. S1D). Following ligand internalisation, cell-surface biotin was removed by treatment with the reducing agent, 2-mercaptoethanesulfonic acid sodium salt (MESNa), while internalised cell-surface proteins were protected and remained biotinylated. This allowed the amount of internalised wild-type and mutant Dome to be quantitated. As has been demonstrated previously for Dome (Ren et al., 2015), we observed ligand-independent internalisation of Dome (Fig. S1E). We found that mutation of the entire di-Leu cassette to AAASKAA (defined from now on as Dome^{allA}) inhibited internalisation of Dome. Mutation of the di-Leu motif alone (Dome^{LL985AA}–FLAG) did not significantly reduce internalisation. Using site-directed mutagenesis in which we progressively replaced elements of the putative cassette, we established that Glu980 and ^{985}LL^{986} together represent essential residues required for Dome internalisation (Fig. 1D,E). Mutation of Glu980 alone did not significantly affect Dome internalisation (Fig. S1F,G). Although uptake of Dome $^{E980G/LL985AA}$–FLAG was significantly inhibited (∼66%), the effect on internalisation was less than that observed for the Dome^{allA}–FLAG mutant, suggesting that other determinants may also be present

Journal of Cell Science (2020) 133, jcs246199. doi:10.1242/jcs.246199

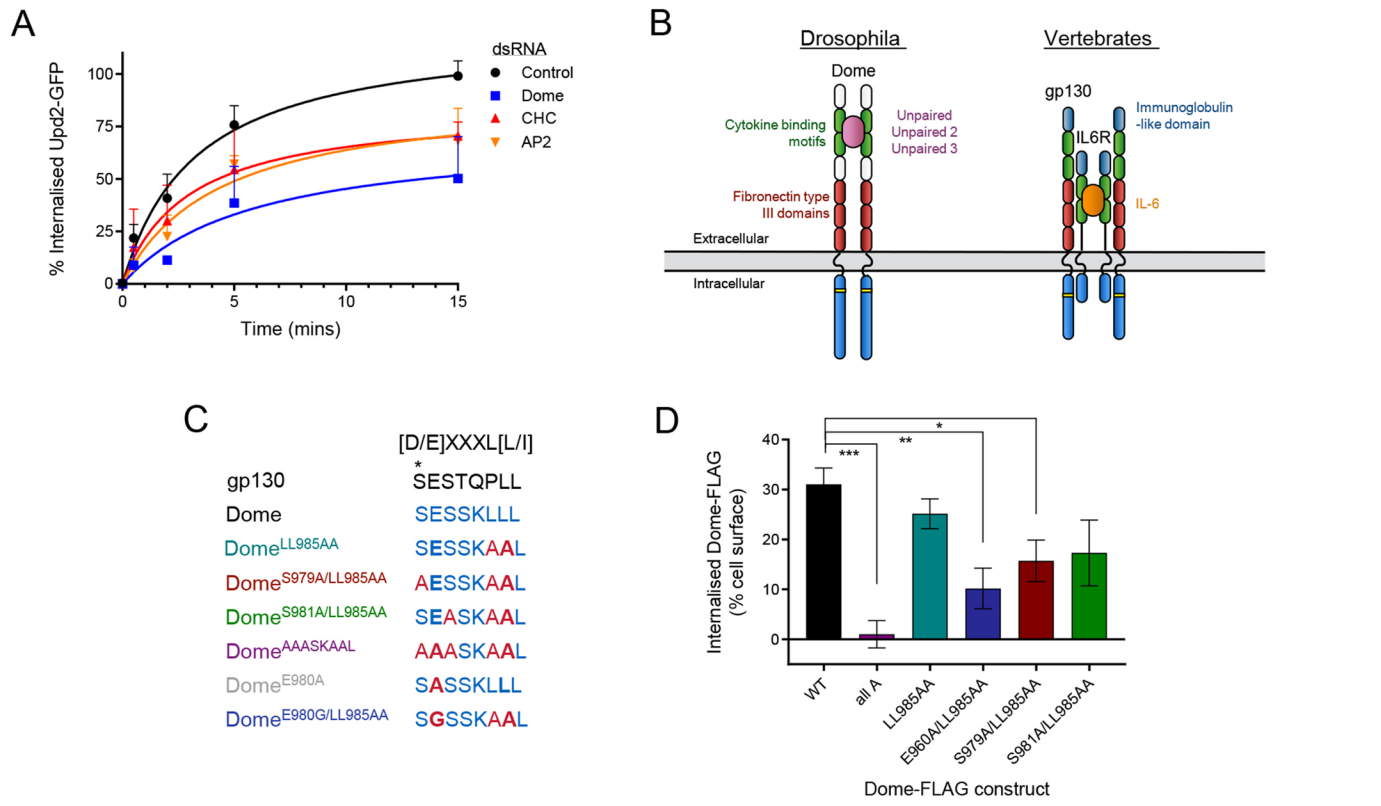

Fig. 1. Uptake of Upd2–GFP into S2R+ cells is Dome-, clathrin- and AP2-dependent. (A) S2R+ cells were treated for 5 days with control, clathrin (CHC), AP2, or Dome dsRNA. Cells were incubated with 20 nM Upd2–GFP for the indicated times at 25°C. Following acid washes, cell lysates were analysed with an anti-GFP ELISA. Internalised Upd2–GFP is expressed as a percentage of the total amount internalised at 15 min. Data represent mean±s.d. of two independent experiments. Data were fitted using the non-linear least-squares fit in GraphPad Prism. (B) Schematic of *Drosophila* Dome and the vertebrate gp130–IL6R complex. (C) A di-Leu cassette in the cytoplasmic tail of gp130 and Dome, and mutants generated to investigate internalisation motifs. Note, Dome^{AAASKAAL} is referred to as Dome^{allA} in the text. X indicates any amino acid. Asterisk indicates Ser780 of gp130, previously shown to modulate rapid internalisation of IL-6 (Dittrich et al., 1996). (D) Quantitation of internalisation of wild-type and mutant Dome–FLAG, showing the percentage of cell-surface receptor that is internalised after 15 min at 25°C. The background signal of biotinylated cell-surface Dome–FLAG after 0 min endocytosis and MESNa treatment was subtracted, and internalised Dome–FLAG was then calculated as a percentage of total cell-surface Dome–FLAG prior to MESNa treatment. Graphs represent mean±s.e.m. for at least three independent experiments (Dome$^{E980A/LL985AA}$, n=3; all other mutants, n≥4). *P<0.05; **P<0.01; ***P<0.001 (parametric unpaired Student's t-test). (E) Sample immunoblot of total lysates and streptavidin pulldowns from cells transfected with Dome^{WT}–FLAG, Dome^{allA}–FLAG, Dome^{LL985AA}–FLAG, Dome$^{E980G/LL985AA}$–FLAG, Dome$^{S979A/LL985AA}$–FLAG or Dome$^{S981A/LL985AA}$–FLAG for 48 h prior to cell-surface biotinylation and incubation at 25°C for the times indicated with or without Upd2–GFP and MESNa treatment. Western blots were probed with antibodies as indicated and molecular mass markers in kDa are shown.

within the sequence that are important for Dome internalisation (Fig. 1D,E). Taken together, these results identify a di-Leu-containing cassette as being essential for Dome internalisation.

Dome signalling is regulated by endocytosis

Dome signalling is known to be regulated by endocytosis in Kc$_{167}$ cells (Müller et al., 2008; Vidal et al., 2010) and *in vivo* (Devergne et al., 2007). To test whether it is similarly regulated in S2R+ cells, we measured the expression of the exogenous reporter *10×STAT–Luciferase,* which expresses the firefly luciferase enzyme under the control of a minimal promoter downstream of ten STAT92E binding sites (Baeg et al., 2005). As expected, this reporter is activated in S2R+ cells by exogenous Upd2–GFP, in a dose-dependent manner (Fig. 2A), indicating that these cells express the JAK/STAT pathway components required for activation. We next measured Upd2–GFP-dependent *10×STAT–Luciferase* reporter activity in control cells and those expressing FLAG-tagged wild-type Dome (Dome ^{wt}–FLAG) or Dome^{allA}–FLAG (Fig. 2B). Although expression of

Journal of Cell Science (2020) 133, jcs246199. doi:10.1242/jcs.246199

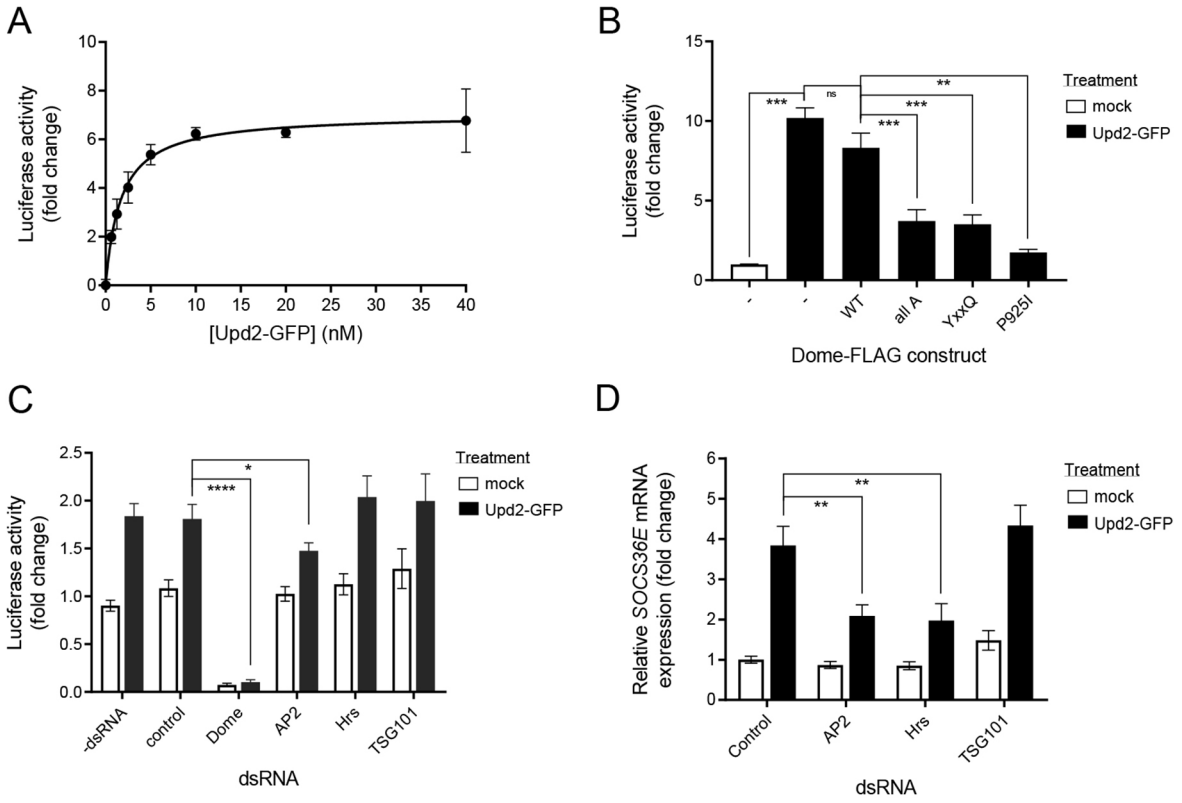

Fig. 2. Endocytosis regulates Dome target gene expression. (A) Expression of *10×STAT–Luciferase* reporter is Upd2–GFP dependent. S2R+ cells were transfected with an actin-driven Renilla luciferase (RL) and *10×STAT–Luciferase* (FL) reporter construct for 6 h and then treated with varying concentrations of Upd2–GFP for 30 min, followed by incubation for 18 h in fresh medium before bioluminescence was measured. Graph represents mean±s.d. of two experiments, each performed in triplicate. (B) Mutation of Dome internalisation motifs inhibits Upd2–GFP-induced *10×STAT–Luciferase* reporter activation. S2R+ cells were transfected with RL and FL reporters alongside pAc5.1 (–), Dome^{WT}–FLAG (WT), Dome^{allA}–FLAG (all A), Dome$^{Y966A/Q969A}$–FLAG (YxxQ) or Dome ^{P925I}–FLAG (P925I). Cells were stimulated with 0.75 nM Upd2–GFP for 30 min, then incubated in fresh medium for 18 h. Luciferase activity (FL/RL) is presented as a fold change compared to mock-treated cells transfected with pAc5.1. Graph represents mean±s.e.m. for four independent experiments, each conducted in triplicate. $^{**}P\leq0.01$; $^{***}P\leq0.001$; ns, not significant (parametric, unpaired Student's *t*-test). (C) S2R+ cells were transfected with RL and FL for 6 h prior to treatment with dsRNA targeting Dome, AP2, Hrs or TSG101, or with control (non-targeting) dsRNA, and incubated for 5 days. Cells were treated with Upd2–GFP for 18 h and then bioluminescence was measured. Luciferase activity (FL/RL) is normalised to control, mock-treated, cells. Graph represents mean±s.e.m. for four experiments, each conducted in triplicate. Parametric, unpaired Student's *t*-tests were carried out to compare Upd2–GFP-stimulated samples only. $^{*}P\leq0.05$; $^{****}P\leq0.0001$. (D) S2R+ cells were treated with dsRNA against AP2, Hrs and TSG101 as well as non-targeting (control) dsRNA for 5 days. Cells were incubated with 3 nM Upd2–GFP for 2.5 h prior to RNA extraction. *socs36* mRNA levels were normalised to that of the reference gene *Rpl32*, and are presented as fold change compared to mock-treated control samples. Results are expressed as mean±s.e.m. for three independent experiments, each conducted in triplicate. Parametric, unpaired Student's *t*-test was carried out to compare Upd2–GFP-stimulated samples only. $^{**}P\leq0.01$.

Dome^{WT}–FLAG did not significantly affect signalling, expression of Dome^{allA}–FLAG had a strong dominant-negative effect on Upd2–GFP-mediated pathway stimulation. This effect was comparable to the level observed in cells expressing Dome$^{Y966A/Q969A}$–FLAG and Dome^{P925I}–FLAG, mutants which have been previously reported to have reduced signalling because of their inability to bind STAT92E (Stahl and Yancopoulos, 1994) and Hop (Fisher et al., 2016), respectively. Levels of expression of the transfected proteins are shown in Fig. S2A. Taken together, these data demonstrate that Dome mutants that cannot be internalised also alter JAK/STAT signalling and are consistent with a model where activation of *10×STAT–Luciferase* by Upd2–GFP is dependent on Dome internalisation.

Endocytosis generates qualitatively different transcriptional outputs

To further explore a role for endocytosis in regulating signalling downstream of Dome, we asked whether knocking down components of the endocytic machinery might differentially affect expression of Dome target genes. We therefore examined the expression of the *10×STAT–Luciferase* reporter and the endogenous target genes *socs36E* and *lama* (Flaherty et al., 2009; Karsten et al., 2002) in cells treated with dsRNA to knock down endocytic components. We targeted AP2, an adaptor whose knockdown is predicted to result in accumulation of receptors at the cell surface (Robinson, 2004); Hrs, an adaptor whose knockdown is likely to result in accumulation of ubiquitylated receptors in early endosomes; and TSG101, which is required for the sorting of receptors into intraluminal vesicles and whose knockdown is likely to lead to an accumulation of receptors on the limiting membrane of late endosomes (Henne et al., 2013). Treating cells with dsRNA to knockdown Dome (levels of Dome mRNA were reduced by ∼90%; Fig. S1B) resulted in almost complete abolition of *10×STAT–Luciferase* expression, demonstrating that both background, and Upd2–GFP-stimulated, reporter activation are receptor dependent (Fig. 2C). In the absence of exogenous ligand, activation of *10×STAT–Luciferase* in cells treated with dsRNA targeting AP2, Hrs or TSG101 was, however, unchanged compared to cells treated

Journal of Cell Science (2020) 133, jcs246199. doi:10.1242/jcs.246199

with control dsRNA (Fig. 2C). We speculate that this ligand-independent activation is due to expression of ligands and growth factors that may crosstalk with the JAK/STAT pathway in S2R+ cells (Cherbas et al., 2011). By contrast, knockdown of AP2 significantly reduced ligand-dependent *10×STAT–Luciferase* activation, whereas knockdown of Hrs or TSG101 had no effect. This indicates that activation of this reporter requires delivery of activated Dome either to, or beyond, an AP2-positive endocytic compartment but prior to an Hrs-positive endosomal compartment. We also examined an endogenous target of Dome, *socs36E* (Stec et al., 2013) and found that, in contrast to *10×STAT–Luciferase* expression, knockdown of both AP2 and Hrs inhibited *socs36E* mRNA expression, whereas knockdown of TSG101 had no effect (Fig. 2D). This indicates that activated Dome must be trafficked to an Hrs-positive compartment, or beyond, to allow downstream pathway activation to trigger *socs36E* transcription. Taken together, these results indicate that the location of the activated Upd2–Dome complexes within the endocytic pathway can lead to qualitatively different signalling outputs. It is important to note that not all Dome target genes are regulated by endocytosis. For example, expression of *lama*, a well-characterised target of STAT92E (Flaherty et al., 2009), was unaffected when endocytosis was perturbed, suggesting that expression of this target gene mRNA can be driven by activated Upd2–Dome complexes that are located on the plasma membrane (Fig. S2B).

Phosphorylation of STAT92E is necessary, but not sufficient, for transcription of some JAK/STAT targets

Upon ligand activation of Dome, STAT92E is phosphorylated by Hop at a conserved Tyr residue (Y704) (Yan et al., 1996). This residue is conserved across all vertebrate STATs, and its phosphorylation is essential for canonical STAT activity and target expression. We therefore asked whether Tyr704 phosphorylation of STAT92E was sensitive to endocytic regulation. One approach to assaying STAT92E phosphorylation utilises its change in electrophoretic mobility on SDS–PAGE gels (Shi et al., 2008), caused by changes in charge and conformation that occur following phosphorylation (Mao et al., 2005; Wenta et al., 2008). Using this experimental approach, we observed an Upd2-dose-dependent change in the electrophoretic mobility of STAT92E following ligand stimulation (Fig. 3A,B), which was

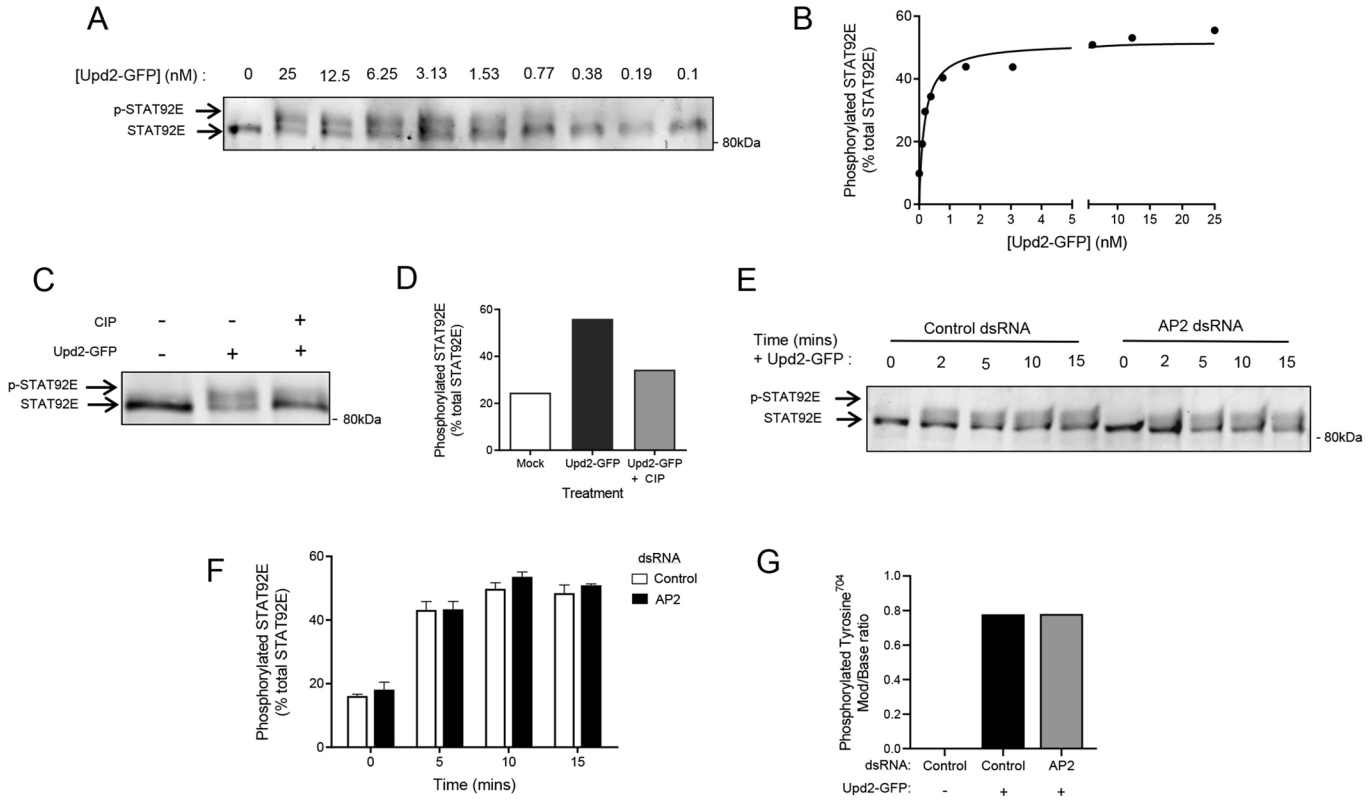

Fig. 3. Tyr704 phosphorylation of STAT92E is independent of endocytic regulation. (A) Western blot showing that Upd2–GFP causes a concentration-dependent band mobility shift, indicative of phosphorylation of STAT92E. The positions of the non-phosphorylated and phosphorylated (p-STAT92E) forms are indicated on the blot. (B) Graph showing quantitation of phosphorylated STAT92E as a function of Upd2–GFP concentration. Phosphorylated STAT92E is expressed as a precentage of total STAT92E. (C) S2R+ cells were treated with 3 nM Upd2–GFP for 10 min, and lysates incubated with anti-STAT92E antibodies. Immunoprecipitated protein was then treated with calf intestinal phosphatase (CIP), then analysed by SDS–PAGE and immunoblotting with anti-STAT92E antibodies. p-STAT92E and STAT92E are indicated by arrows. (D) Quantitation of p-STAT92E as a percentage of total STAT92E in cells with or without Upd2–GFP and CIP treatment. (E) Representative immunoblot of control and AP2-knockdown S2R+ cells treated with 3 nM Upd2–GFP at 25°C for the indicated times. Cells were treated with targeting dsRNA and incubated for 5 days at 25°C. Total protein extract was analysed by SDS–PAGE and immunoblotted with anti-STAT92E antibodies. (F) Quantification of STAT92E phosphorylation after AP2 knockdown. Phosphorylated STAT92E is expressed as percentage of total STAT92E. Results are expressed as mean±s.e.m. from four independent experiments. Using a Student's *t*-test, there are no statistically significant differences between control and AP2-knockdown samples. (G) Upd2-dependent phosphorylation of Tyr704 is unchanged following dsRNA-mediated knockdown of AP2. S2R+ cells treated with control and AP2 dsRNA were transfected with STAT92E–GFP and treated with 3 nM Upd2–GFP for 75 min. Cells were lysed and incubated with GFP-trap beads prior to preparation for mass spectrometry analysis. Histograms present the Mod/Base (phosphorylated:unmodified peptide abundance) ratio of the Y704 phosphorylation site from STAT92E–GFP samples calculated by MaxQuant software in all conditions. Data shown for n=1.

Journal of Cell Science (2020) 133, jcs246199. doi:10.1242/jcs.246199

reversed by phosphatase treatment (Fig. 3C,D). Strikingly, perturbation of the endocytic pathway by knockdown of AP2 (Fig. 3E,F), or Hrs or TSG101 (Fig. S3), did not affect the temporal dynamics of STAT92E phosphorylation, a finding that was also confirmed by mass spectrometry (Fig. 3G; data available via ProteomeXchange PXD020719). These data demonstrate that phosphorylation on Tyr704 of STAT92E is not regulated by endocytosis and that other mechanisms must be responsible for the pathway's sensitivity to endocytic regulation.

STAT92E–GFP nuclear import is not affected by knockdown of endocytic components

Canonical JAK/STAT pathway signalling requires nuclear import of the STAT92E transcription factor to activate gene expression. We therefore investigated whether knockdown of AP2 impaired translocation of STAT92E into the nucleus. Nuclear accumulation could be visualised in S2R+ cells transfected with STAT92E–GFP. In the absence of ligand there appeared to be low levels of STAT92E–GFP in the nucleus. This is consistent with reports that STATs shuttle between the nucleus and cytoplasm in a phosphorylation-independent manner and that unphosphorylated nuclear STATs can perform non-canonical functions (Brown and Zeidler, 2008). The levels of nuclear STAT92E–GFP we observed in the absence of Upd2 is also in keeping with reports of GFP-tagged proteins entering the nucleus independently of a nuclear localisation signal (Seibel et al., 2007). When cells were treated with Upd2–GFP (Fig. 4A,B), a maximum accumulation was reached after 30 min stimulation. This is comparable to the nuclear accumulation of mammalian STATs (McBride et al., 2000) and the time-point at which STAT92E phosphorylation is maximal (data not shown). Consistent with previous studies (Begitt et al., 2000; Schindler et al., 1992), mutation of STAT92E Tyr704 (Y704F), to prevent phosphorylation, abolished nuclear accumulation (Fig. 4C). Although knockdown of Dome almost completely abolished nuclear accumulation of STAT92E–GFP, knockdown of either AP2 or Hrs had no significant effect, indicating that endocytic trafficking of Upd2–Dome does not regulate nuclear accumulation of STAT92E (Fig. 4D). This demonstrates that the loss of target gene expression following AP2 and Hrs knockdown is not likely to be the result of a defect in the translocation of STAT92E into the nucleus.

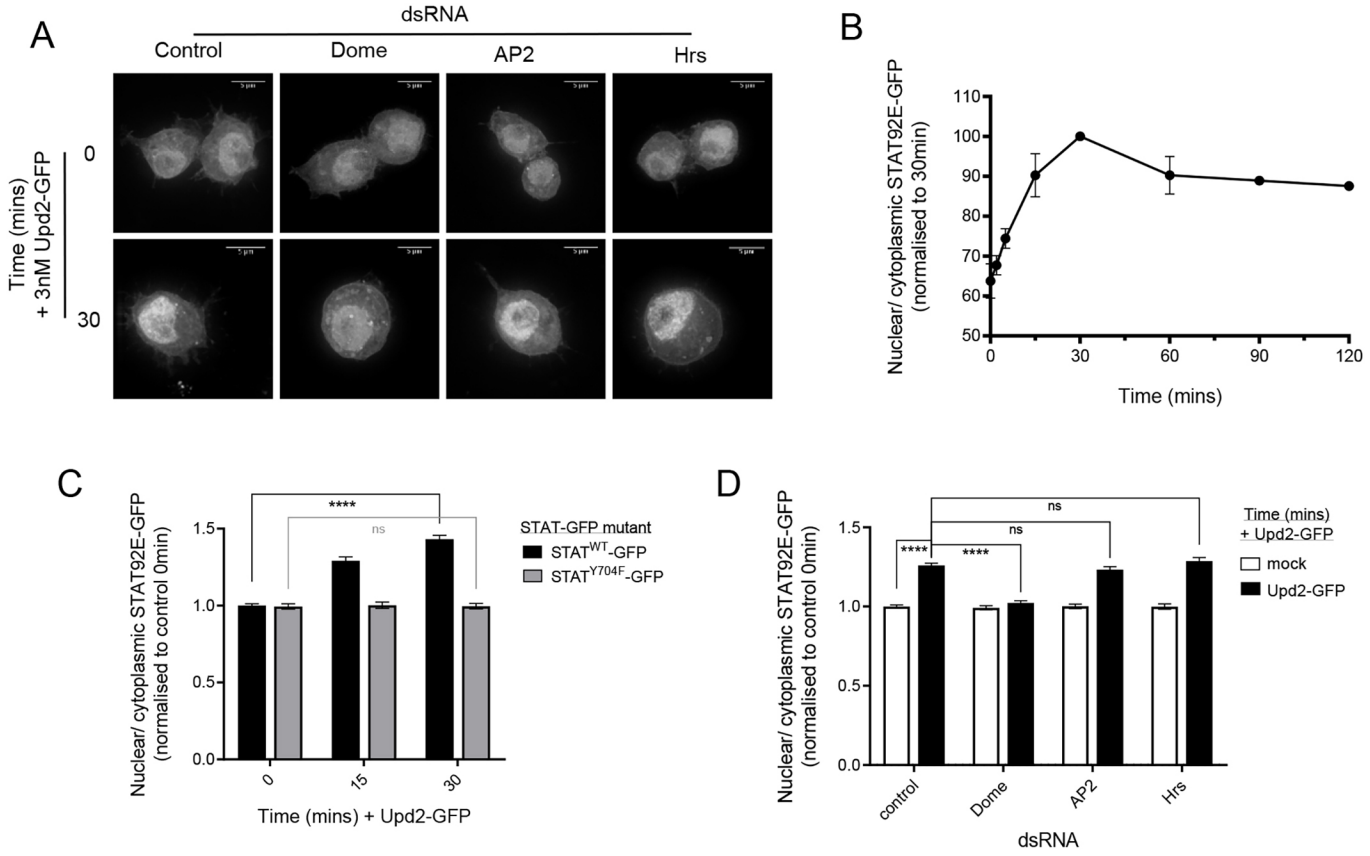

Fig. 4. Upd2-dependent nuclear translocation of STAT92E requires Tyr704 phosphorylation but is independent of endocytosis. (A) Representative images of cells treated with control dsRNA or dsRNA targeting Dome, AP2 or Hrs for 5 days and transfected with STAT92E^{WT}–GFP (on day 3) and treated with 3 nM Upd2–GFP for 0 or 30 min. Scale bars: 5 µm. (B) Timecourse of nuclear accumulation of STAT92E–GFP following treatment with Upd2–GFP. Nuclear signal was divided by cytoplasmic signal and expressed as a percentage of nuclear STAT92E–GFP after 30 min. Data are presented as mean±s.d. for at least two independent experiments where >15 cells were examined per experiment. (C) Quantitation of nuclear versus cytoplasmic STAT92E^{wt}–GFP and STAT92E^{Y704F}–GFP following treatment of cells with Upd2–GFP for the times indicated. Nuclear signal was divided by cytoplasmic signal and normalised to the signal at 0 min in control cells. Data are presented as mean±s.e.m. where at least 80 cells were imaged in total from three independent experiments. (D) Quantitation of nuclear STAT92E–GFP versus cytoplasmic STAT92E–GFP following treatment of cells with control dsRNA or dsRNA targeting Dome, AP2 or Hrs and either treatment with Upd2–GFP or mock treatment. Nuclear signal was divided by cytoplasmic signal and normalised to the signal in control mock-treated cells at 0 min. Data are presented as mean±s.e.m. for three independent experiments where at least 20 cells were imaged per condition per experiment. ****$P \leq 0.0001$; ns, not significant (parametric, unpaired Student's *t*-test).

Journal of Cell Science

Journal of Cell Science (2020) 133, jcs246199. doi:10.1242/jcs.246199

Thr702 phosphorylation is essential for STAT92E activity

Given that Y704 phosphorylation is necessary but not sufficient for STAT92E-driven pathway gene expression, we wanted to investigate whether other posttranslational modifications of STAT92E might be associated with pathway activation. We expressed STAT92E–GFP in S2R+ cells, stimulated them with Upd2–GFP and subjected samples isolated using GFP–TRAP beads to mass spectrometry analysis. In addition to Tyr704, this analysis identified Thr47, Ser227 (Fig. 5A) and Thr702 (with lower confidence) on STAT92E as being phosphorylated (data available via ProteomeXchange with identifier PXD020719). We therefore decided to test the potential physiological relevance of these newly identified phosphorylation sites using an S2R+ cell line lacking endogenous STAT92E. We used CRISPR-Cas9 to engineer STAT92E-negative S2R+ cells, demonstrating that the cell line no longer had detectable STAT92E by western blotting (Fig. S4A) and T7 endonuclease assay (Fig. S4B) and was no longer able to activate *10×STAT–Luciferase* in response to Upd2–GFP treatment (Fig. 5B). As expected, expression of wild-type STAT92E was able to rescue both Upd2–GFP-dependent and -independent *10×STAT–Luciferase* activity (Fig. S4C) in these STAT92E-negative cells, whereas ligand-dependent *10×STAT–Luciferase* activity was further enhanced by expression of $STAT92E^{K187R}$, a mutant form of STAT92E that cannot be SUMOylated and that has previously been shown to increase luciferase activity (Grönholm et al., 2010). Taken together, these results demonstrate the utility of the STAT92E-negative S2R+ cells for rescue experiments (Fig. S4C).

We next generated mutant forms of STAT92E lacking both known and candidate phosphorylation sites (T47V, S227A, T702V and Y704F), expressed them in STAT92E-negative S2R+ cells and measured their ability to activate *10×STAT–Luciferase*. Following ligand stimulation with 0.75 nM Upd2–GFP, $STAT92E^{T47V}$, $STAT92E^{S227A}$ and $STAT92E^{WT}$ resulted in comparable levels of *10×STAT–Luciferase* activation, whereas cells expressing $STAT92E^{T702V}$ and $STAT92E^{Y704F}$ showed no activation (Fig. 5C). This indicates that phosphorylation of Thr702 as well as Tyr704, but not Thr47 or Ser227, is required for JAK/STAT signalling.

Phosphomimetic forms of STAT92E rescue signalling

To further explore the role of Thr702 phosphorylation in STAT92E-mediated gene activation, we generated phosphomimetic mutants of Thr702 ($STAT92E^{T702D}$, $STAT92E^{T702E}$) and tested their effects on

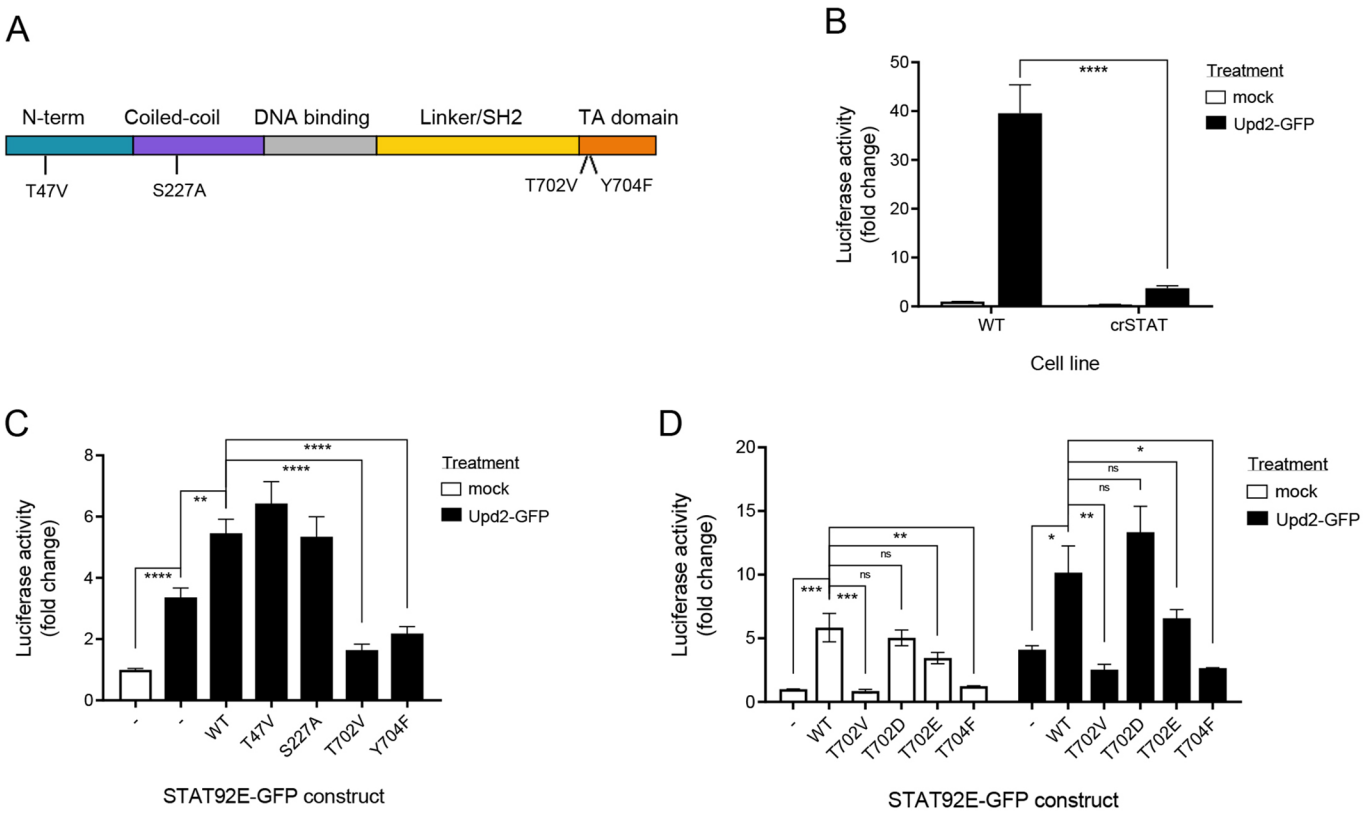

Fig. 5. Phosphorylation on Thr702 of STAT92E is essential for its function. (A) Schematic of STAT92E indicating domains, Tyr704 and novel phosphorylation sites that were identified by mass spectrometry. (B) Control cells (WT) or cells lacking STAT92E (crSTAT) were transfected with pAc-Ren (RL) and *10×STAT–Luciferase* (FL) reporter for 24 h. Cells were stimulated with 3 nM Upd2–GFP for 30 min or mock-treated, and then incubated in fresh medium for 18 h. Luciferase activity (FL/RL) is expressed as a fold change compared to mock-treated cells transfected with pAc5.1. Graph represents mean±s.e.m. of three independent experiments, each performed in triplicate. ****$P\leq0.0001$ (parametric, unpaired Student's *t*-test). (C) STAT92E mutants that cannot be phosphorylated, $STAT92E^{T702V}$ and $STAT92E^{Y704F}$, inhibit Upd2–GFP-dependent signalling. crSTAT cells were transfected with pAc-Ren, *10×STAT–Luciferase*, or pAc5.1 (–), and with wild-type or mutant STAT92E–GFP as indicated. Cells were mock-treated or stimulated with 0.75 nM Upd2–GFP for 30 min and then incubated in fresh medium for 18 h. Data are mean±s.e.m. from three independent experiments, each performed in triplicate and normalised to the signal in cells transfected with pAc5.1. **$P\leq0.01$; ****$P\leq0.0001$ (parametric, unpaired Student's *t*-test). (D) Phosphomimetic forms of STAT92E rescue inhibitory effects of T702V on Upd2–GFP-dependent signalling. crSTAT cells were transfected with pAc-Ren, *10×STAT–Luciferase*, or pAc5.1 (–), and with wild-type or mutant STAT92E–GFP as indicated. Cells were mock-treated or stimulated with 0.75 nM Upd2–GFP for 30 min, then incubated in fresh medium for 18 h. Luciferase activity (FL/RL) is expressed as a fold change compared to mock-treated cells transfected with pAc5.1 (–). Data is expressed as mean±s.e.m. from three independent experiments. *$P\leq0.05$; **$P\leq0.01$; ***$P\leq0.001$; ns, not significant (parametric, unpaired Student's *t*-test).

Journal of Cell Science (2020) 133, jcs246199. doi:10.1242/jcs.246199

activation of the *10×STAT–Luciferase* reporter. Using the STAT92E-negative S2R+ cell assays, we first showed that expression of 'loss-of-phosphorylation' mutants $STAT92E^{T702V}$ and $STAT92E^{Y704F}$ did not stimulate reporter activity above background levels (Fig. 5D). By contrast, expression of either phosphomimetic mutant, $STAT92E^{T702D}$ or $STAT92E^{T702E}$, was sufficient to increase both ligand-dependent and ligand-independent *10×STAT–Luciferase* expression, with $STAT92E^{T702D}$ more effective in both cases. Taken together, we have thus identified a novel posttranslational modification of STAT92E that is essential for triggering transcriptional activity in this assay.

Phosphorylation of Thr702 is required for Tyr704 phosphorylation

We next asked whether Thr702 phosphorylation is required for nuclear translocation of STAT92E and found that Upd2–GFP does not stimulate $STAT92E^{T702V}$ translocation into the nucleus (Fig. 6A, B). Using mass spectrometry, we found that $STAT92E^{T702V}$ showed a substantial reduction in Tyr704 phosphorylation (Fig. 6C; data available via ProteomeXchange with identifier PXD020719). This indicates that phosphorylation of Thr702 is essential for efficient phosphorylation of Tyr704, which, in turn, is essential for the bulk of canonical JAK/STAT gene expression.

DISCUSSION

In this work we have explored regulatory mechanisms of JAK/STAT signalling following Upd2-dependent Dome activation in *Drosophila* S2R+ cells. We have identified an evolutionarily conserved internalisation motif in the cytoplasmic tail of Dome. We have demonstrated that internalisation and endocytic trafficking of activated Dome allows for compartmentalised signalling to regulate subsets of *Drosophila* JAK/STAT transcriptional targets, through a mechanism that is independent of Tyr704 phosphorylation of STAT92E. We have also demonstrated that phosphorylation of Thr702 is essential for Tyr704 phosphorylation of STAT92E, its translocation to the nucleus and its activity as a transcription factor.

It has been shown that Dome enters cells by CME *in vivo* in *Drosophila* (Devergne et al., 2007) and *in vitro* in Kc_{167} cells (Müller et al., 2008; Vidal et al., 2010). Our results also support a role for CME in Dome uptake in S2R+ cells, because dsRNA-mediated knockdown of CHC and AP2 reduced Upd2–GFP internalisation. There are a number of defined motifs that allow the inclusion of transmembrane receptors into clathrin-coated pits, through interactions with adaptor molecules such as AP2. A di-Leu motif is one such motif, which is well documented to bind to the α–σ2 hemicomplex of AP2 (Doray et al., 2007; Kelly et al., 2008). In this work, we have demonstrated that such a motif is part of a cassette that is essential for efficient internalisation of Dome. Interestingly, a di-Leu-containing cassette is also required for the internalisation of gp130, the closest vertebrate homologue of Dome and the co-receptor for IL-6R, which is necessary for IL-6R internalisation (Dittrich et al., 1996). Similar to gp130, mutation of the di-Leu motif alone in Dome was insufficient to completely abolish internalisation. In the case of gp130, a Ser residue upstream of the di-Leu motif was also shown to be involved in rapid internalisation. We found that mutation of the equivalent Ser, in combination with mutation of the di-Leu motif, further reduced Dome internalisation, although still not to the same extent as in the $Dome^{allA}$ mutant. An acidic residue (Glu or Asp) at the −4 position is commonly found adjacent to di-Leu motifs, and its mutation has previously been shown to drastically decrease binding to the α–σ2 hemicomplex of AP2 (Doray et al., 2007). Mutation of this charged residue alone had no effect on receptor internalisation, whereas mutation of both the Glu and di-Leu residues reduced internalisation by ∼66% compared to internalisation of $Dome^{WT}$. This suggests that, although the Glu and di-Leu are important, other residues may also influence Dome internalisation. It also points to an important evolutionary conservation in mechanisms of Dome internalisation that is in line with the conservation of JAK/STAT pathway components across species.

Our results support a role for CIE, in addition to CME, in uptake of activated Dome in S2R+ cells. While dsRNA-mediated knockdown of CHC and AP2 inhibits internalisation of Upd2–GFP bound to Dome, the extent of inhibition depends on the concentration of the Upd2–GFP ligand. At low concentrations (3 nM) of Upd2–GFP, there is an absolute requirement for CHC and AP2, whereas at higher concentrations (20 nM), uptake of Upd2–GFP bound to Dome in cells treated with dsRNA targeting CHC and AP2 is inhibited by ∼50% compared to cells treated with dsRNA targeting Dome. This is consistent with studies in *Drosophila* where uptake of Notch and Delta through different endocytic pathways (CME and CIE) leads to delivery to different endosomal compartments and differential signalling, with the balance of flux between these pathways allowing cells to respond to different environmental conditions (Shimizu et al., 2014). Similarly, in mammalian cells, activated receptor tyrosine kinases, such as TGF-β receptors and EGFR, can be taken up by CME and CIE, with CME being favoured at lower ligand concentrations (Di Guglielmo et al., 2003; Sigismund et al., 2005). As with Notch signalling, the route of entry of the receptors can determine signalling outcome and receptor fate (Sigismund et al., 2013; Vander Ark et al., 2018). The concept of endocytosis modulating Dome target gene expression in different cells and tissues is supported by previous *in vitro* and *in vivo* studies (Devergne et al., 2007; Silver et al., 2005; Vidal et al., 2010). Our experiments, which have focussed on CME of activated Dome, indicate that endocytosis also regulates a subset of Dome signalling in S2R+ cells. Mutation of the internalisation motif not only prevented Dome uptake but also prevented Dome activation of *10×STAT–Luciferase*, consistent with a role for endocytosis in activation of target genes. It is noteworthy that we observed constitutive internalisation and recycling of Dome in the absence of ligand, similar to that observed for other cytokine receptors in mammalian cells (Thiel et al., 1998). Regulation of constitutive recycling provides cells with a mechanism to control cell-surface levels of receptor, which in turn will impact on the magnitude of signalling (Moore et al., 2018).

Strikingly, we have demonstrated that endocytosis of Dome allows an additional level of regulatory control, in that delivery to distinct endosomal populations can further affect signalling outcome. Endocytosis is not required for expression of all genes, for example, *lama* is still expressed even when components of the endocytic machinery are ablated with dsRNA. By contrast, expression of *10×STAT–Luciferase* requires delivery to, or beyond, an AP2-positive compartment, and expression of *socs36E* only occurs when activated Dome has trafficked through an Hrs-positive compartment, but before it has reached a TSG101-positive compartment (Fig. 6D). Our data thus demonstrate that qualitatively different signalling outputs can occur depending on the location of the activated receptor within the endocytic pathway. This strongly supports the concept that the rate at which receptors, in this case Dome, move through the pathway (endocytic flux) is key for signalling outputs and will have profound effects on downstream cell behaviours. This is consistent with studies of EGFR signalling,

Journal of Cell Science (2020) 133, jcs246199. doi:10.1242/jcs.246199

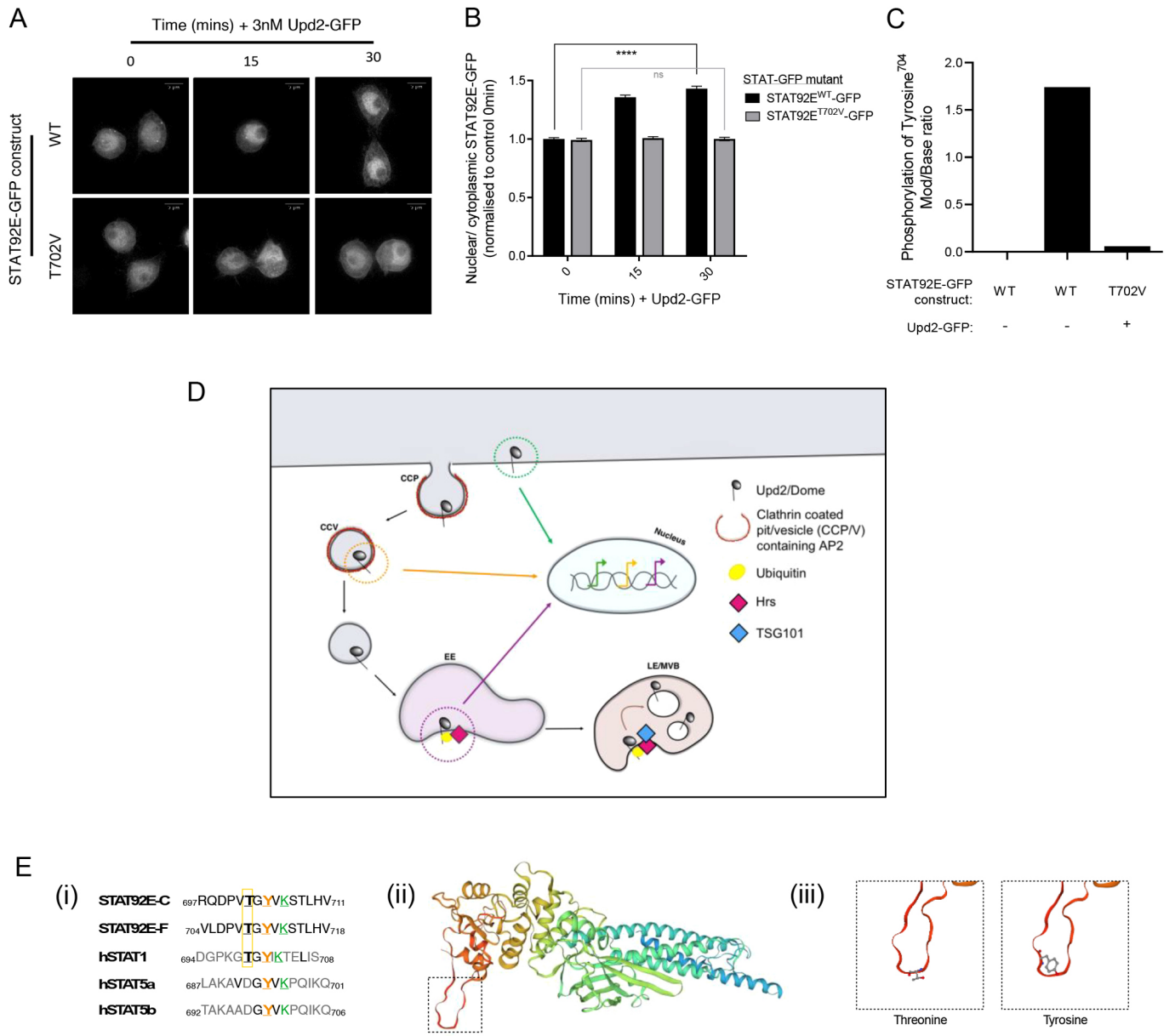

Fig. 6. Phosphorylation of Thr702 is essential for Tyr704 phosphorylation. (A) T702V mutation prevents STAT92E–GFP nuclear translocation in response to ligand. Representative images of cells lacking STAT92E (crSTAT) transfected with either STAT92E^{WT}–GFP or STAT92E^{T702V}–GFP and treated with 3 nM Upd2–GFP for 0, 15 or 30 min. Scale bar: 5 µm. (B) Nuclear signal was divided by cytoplasmic signal and normalised to the signal in control cells at 0 min. Data is presented as mean±s.e.m. for three independent experiments, where at least 30 cells were imaged per condition per experiment. ****$P\leq0.0001$; ns, not significant (parametric, unpaired Student's *t*-test). (C) Mutation of Thr702 reduces phosphorylation on Tyr704. S2R+ cells were transfected with STAT92E^{WT}–GFP or STAT92E^{T702V}–GFP 2 days prior to treatment with 3 nM Upd2–GFP for 75 min. Cells were lysed and incubated with GFP-trap beads prior to preparation for mass spectrometry analysis. Histograms present the Mod/Base (phosphorylated:unmodified peptide abundance) ratios of the Y704 phosphorylation site from STAT92E^{WT}–GFP and STAT92E^{T702V}–GFP, as calculated by MaxQuant software. Data shown for n=1. (D) Compartmentalised signalling regulates expression of JAK/STAT targets. Diagram depicting how movement of the Upd2–Dome complex along the endocytic pathway regulates differential gene expression. At the cell surface, activated Dome can result in transcription of a subset of target genes (e.g. *Iama*, shown in green). Following uncoating of clathrin and AP2 from clathrin-coated vesicles, other genes can be activated (e.g. *Luciferase*, shown in orange). Hrs selects ubiquitylated cargo for incorporation into intraluminal vesicles, but activated Dome can still signal to activate other genes (e.g. *socs36E*, shown in purple) before TSG101 results in incorporation of Upd2–Dome into invaginations of the endosomal membrane to form intraluminal vesicles, which results in termination of signalling. EE, early endosome; LE, late endosome; MVB, multi-vesicular body. (E) Thr702 conservation and location within STAT1 crystal structure. (i) Alignment of sequences surrounding the conserved Tyr in STAT92E-C (C isoform), STAT92E-F (long isoform), human STAT1, STAT5a and STAT5b. The conserved Tyr is highlighted in orange, and a conserved Lys highlighted in green. The Thr residue is in a yellow box. (ii) Crystal structure of STAT1 (PDB ID 1bf5). Dashed box indicates the loop region shown to the right. (iii) Location of the Thr and Tyr residues within the STAT1 crystal structure.

which imply that receptor signalling can modulate the endocytic machinery to determine the rate of receptor flux (Villaseñor et al., 2015). Although mechanistic details for endocytic regulation of signalling are better understood for receptor tyrosine kinases (RTKs) and G-protein-coupled receptors (GPCRs), there is a considerable body of emerging evidence to support a role for endocytic regulation of cytokine receptors in mammalian cells (Cendrowski et al., 2016). Our data are thus consistent with a variety

Journal of Cell Science (2020) 133, jcs246199. doi:10.1242/jcs.246199

of studies in mammalian cells demonstrating an instructive role for endocytosis in JAK/STAT signalling (Cendrowski et al., 2016; Chmiest et al., 2016; German et al., 2011; Kermorgant and Parker, 2008; Marchetti et al., 2006).

In *Drosophila*, STAT92E is the single transcription factor utilised by the JAK/STAT pathway to control expression of many different target genes, which are expressed in a tissue-specific and developmentally-regulated manner. The essential role of Tyr704 phosphorylation in JAK/STAT signalling is well established (Yan et al., 1996). We eliminated the possibility that endocytosis is required for STAT92E phosphorylation by demonstrating that STAT92E is phosphorylated to the same extent when components of the endocytic machinery, such as AP2, are knocked down by dsRNA. More importantly, our data demonstrate that STAT92E Tyr704 phosphorylation, although necessary, is not sufficient for the expression of all Dome target genes. Our data are consistent with previous studies showing that a mutant form of STAT92E that cannot be methylated is hyper-phosphorylated, but has a dominant-negative effect on target gene expression (Karsten et al., 2006).

When the endocytic pathway is disrupted, phosphorylated STAT92E can still translocate into the nucleus, but it is no longer fully signalling competent. This implies that Dome needs to reach a particular endosomal subcompartment or microdomain in order to allow STAT92E to become transcriptionally competent. Of particular interest is the post-Hrs and pre-TSG101 compartment required for *socs36E* expression (Fig. 6D). Hrs is a component of the ESCRT-0 complex, which recognises ubiquitylated signalling cargo destined to be packaged into inward invaginations of the endosomal membrane to form intraluminal vesicles and, ultimately, multivesicular bodies. TSG101 is required for later stages of intraluminal vesicle formation (Vietri et al., 2019). As such, both these components are found within the same limiting membrane. It has been proposed that membrane microdomains of defined composition, containing signalling molecules, must be able to form within endosomal membranes to generate local signalling-competent (signalosome) domains (Shimizu et al., 2014; Teis et al., 2002). Within these specialised signalosomes, STAT92E is likely either to undergo additional posttranslational modifications or to acquire a chaperone protein that facilitates its ability as a transcription factor for a subset of target genes. Support for a Hrs (also known as HGS in mammals) signalosome comes from studies that demonstrate that the Hrs-interacting protein STAM is required for downstream signalling following IL2R activation (Takeshita et al., 1997; Tognon et al., 2014). In mammals, STAMs are phosphorylated in response to a range of cytokines and growth factors (Pandey et al., 2000). The Hrs–STAM complex remains an interesting link between signalling and endocytosis, because it has been shown to have both positive and negative roles in the regulation of RTK signalling in *Drosophila* that are dependent on specific tissue and developmental stages (Chanut-Delalande et al., 2010).

Previous studies in mammalian cells have shown that endosomal location is required for STAT3 activation by activated c-Met (also known as MET), which is classed as a weak activator, and it was proposed that by localising STAT3 activation in endosomes, nuclear import is facilitated (Kermorgant and Parker, 2008). Here, we show the importance of localisation at different points along the endocytic pathway to nuance Dome signalling to allow different signalling outputs, with STAT92E being a target for endocytic regulation.

Mass spectrometry analysis revealed Thr702 as a novel phosphorylation site on STAT92E that is functionally important. Mutation to valine, which is structurally similar but cannot be phosphorylated, prevented STAT92E Tyr704 phosphorylation and nuclear translocation, whereas phosphomimetic forms of Thr702 rescued this phenotype. Alignment (Waterhouse et al., 2018) of STAT92E with the published crystal structure of STAT1 (Chen et al., 1998) suggests that Thr702 and Tyr704 are located in a flexible loop region (Fig. 6E). Phosphorylation is likely to have significant effects on the conformation of this region. Intriguingly, the Thr residue at this position is conserved in STAT1 and is a phosphomimetic residue in STAT5, suggesting that it may play a role in ensuring effective Tyr phosphorylation of STATs across species.

In summary, we have shown that endocytosis regulates JAK/STAT signalling in *Drosophila* S2R+ cells, resulting in qualitatively different signalling outputs. We therefore suggest that the endocytic flux of activated Dome provides a mechanism by which JAK/STAT can regulate different cellular behaviours depending on cell context. In the course of our studies we have shown that although phosphorylation of Tyr704 on STAT92E is necessary, it is not sufficient for expression of some JAK/STAT target genes. Moreover, for some targets, delivery to an endosomal subcompartment is required in order to make STAT92E transcriptionally competent.

MATERIALS AND METHODS

Cell culture

S2R+ cells were cultured at 25°C in Schneider's Insect Tissue Culture medium (Gibco, UK), supplemented with 10% heat inactivated FBS (Sigma-Aldrich, UK.), penicillin (1000 units/ml) and streptomycin (0.1 mg/ml) (Sigma-Aldrich, UK) and 2 mM L-glutamate (Gibco, UK). Cells were grown to confluency in T75 flasks and routinely passaged at a 1:3 dilution every 3–4 days.

Cell transfection

For expression of STAT92E–GFP (Addgene plasmid 126662, deposited by Ron Vale) or Dome–FLAG, cells were seeded a day prior to transfection. They were transfected at a ratio of 2 µg DNA per 1×10^6 cells in a 6-well plate, using Effectene Reagent (Qiagen Ltd, UK) and used 2 days later for experiments. Cells were routinely tested to ensure that they were free of mycoplasma.

Upd2–GFP production

Upd2-GFP conditioned medium was produced essentially as described previously (Wright et al., 2011), with the following modifications: S2R+ cells were seeded at 1×10^6 cells per well of a 6-well plate 1 day prior to transfection. pAct-Upd2–GFP (2 µg per well) was transfected using Effectene Transfection Reagent (Qiagen Ltd, UK) following the manufacturer's instructions. After 2 days, 3 wells of transfected cells were transferred to a T75 flask and incubated for a further 4 days. Cells were centrifuged at 1000 ***g*** for 3 min, and the medium was filtered, aliquoted and snap frozen in liquid N_2, then stored at −80°C. The concentration of Upd2–GFP was determined using an ELISA for GFP (see below). Mock conditioned medium (referred to as mock treatment) was produced by transfecting cells with 2 µg pAc5.1 (Müller et al., 2005) and processed as above.

dsRNA knockdown

dsRNAs were obtained from the Sheffield RNAi Screening Facility, whose dsRNA database is based on the Heidelberg 2 library (Boutros laboratory, DKFZ, Heidelberg, Germany), generated with Next-RNAi (Horn et al., 2010). It is the redesigned, non-off-target-effect library, HD2.0, generated using the software next-RNAi (Horn et al., 2010). Low-complexity regions and sequence motifs that induce off-target effects have been excluded. dsRNA probe sizes vary from 81 to 800 bp covering ∼14,000 protein encoding genes and ∼1000 non-coding genes (∼98.8% coverage). The dsRNA design covers every isoform of each gene and has been optimised for specificity and avoidance of low complexity regions. The following dsRNA amplicons were used: α-adaptin (BKN20148); CHC (BKN20463); Dome (BKN25660); Hrs (BKN27923); and TSG101 (BKN28961). Negative control dsRNA was a mixture of three amplicons targeting

Journal of Cell Science (2020) 133, jcs246199. doi:10.1242/jcs.246199

Caenorhabditis elegans mRNA (BKN70003, BKN70004 and BKN70005). Amplification of dsRNA was carried out using a MEGAscript RNAi Kit (Life Technologies, AM1626), and purified via ethanol precipitation with sodium acetate, followed by resuspension in sterile water.

Cells were seeded 1 day prior to knockdown, and resuspended in serum-free medium on the day of knockdown. The desired number of cells was added to wells already containing dsRNA and incubated for 1 h at 25°C (15 µg of dsRNA plus 1×10^6 cells per well in a 6-well plate). After incubation, an equal volume of fresh medium containing 20% FBS was added. Cells were incubated at 25°C for a total of 5 days before subsequent experiments. Transfection with STAT92E–GFP was performed on day 3 of dsRNA treatment.

Generation of CRISPR S2R+ cell lines

sgRNA were designed to target the N-terminal coding region of STAT92E and showed <1% chance of off-target activity (crispr.mit.edu). Sequences were also verified using NCBI BLAST to eliminate potential off-target hits. The NGG sequence was then removed, and a G was added to the 5′ end of the sgRNA sequence to allow transcription from the U6 promoter in pAc-sgRNA-Cas9 vector (Addgene plasmid 49330, depositied by Ji-Long Liu). sgRNA oligos (Table S1) were cloned into the pAc-sgRNA-Cas9 expression vector following a previously published protocol (Bassett et al., 2014). S2R+ cells were plated at 5×10^5 cells per well in a 12-well plate and transfected with 1 µg pAc-sgRNA-Cas9 construct using Effectene (Qiagen Ltd, UK). After 3 days, puromycin (5 µg ml^{-1}) selection was performed for 7 days before subsequent analysis (Bassett et al., 2014).

To detect Cas9-induced mutations within the genomic DNA of S2R+ CRISPR cell lines, a T7 endonuclease assay was carried out to identify mismatched, heteroduplex DNA. PCR products were first produced by amplifying an ∼1 kb region around the Cas9 cut site in a 50 µl PCR reaction, following a previously published method (Guschin et al., 2010). Following verification of size on agarose gels, PCR products were denatured and annealed to form heteroduplexes in the following reaction: 5–10 µl PCR products, 2 µl NEBuffer 2 (NEB) made up to 19 µl with nuclease-free water. The reaction was heated at in a 95°C heat block for 10 min and allowed to cool to room temperature. 1 µl of T7 endonuclease was then added to reactions and incubated at 37°C for 15 min. The reaction was stopped by addition of 1.5 µl 0.25 M EDTA before running on an agarose gel.

ELISA assay for GFP

The anti-GFP ELISA was performed essentially as described previously (Wright et al., 2011). Briefly, a 96-well high-binding EIA plate (Costar) was coated with 0.0625 µg ml^{-1} goat anti-GFP antibody (Abnova; PAB10341) in 100 mM sodium bicarbonate overnight at 4°C. The plate was washed three times with wash buffer [0.2% (w/v) BSA, 0.5% Triton-X 100 in phosphate-buffered saline (PBS)] and then blocked in the same buffer for 1 h at room temperature. A serial dilution of recombinant GFP (Cellbiolabs; STA-201), starting at 5 ng ml^{-1}, was plated for reference. Samples were incubated for 3 h at 37°C. After washing, the plate was incubated with rabbit anti-GFP (Abcam; Ab290) at 1:20,000 for 2 h at room temperature. After further washes, the plate was incubated with a secondary HRP-linked anti-rabbit antibody (Santa Cruz Biotechnology; sc-2004) at 1:5000 for 1 h at room temperature. Following washing, 200 µl per well of freshly prepared HRP developing solution [0.012% H_2O_2, 0.4 mg ml^{-1} o-phenylenediamine in HRP assay buffer: 51 mM Na_2HPO_4, 27 mM citric acid, pH 5.0, (filtered)] was added to the plate and colour change was observed. To stop the reaction, 50 µl of 2 M H_2SO_4 was added per well, and the absorbance read at 492 nm on a BMG Labtech plate reader.

Endocytosis assays using anti-GFP ELISA

Cells were seeded in a 24-well plate (2×10^5 cells per well) a day prior to the experiment. The medium was replaced with conditioned medium containing established concentrations of Upd2–GFP and incubated at 25°C for various times. Endocytosis was stopped by placing cells on ice and washing twice with ice-cold PBS. Cell-surface ligand was removed by acid washing twice with 0.2 M glycine, 0.15 M NaCl, pH 2.5 for 2 min. Cells were then washed again in PBS before lysis in ELISA lysis buffer [PBS containing 1 mM $MgCl_2$, 0.1% (w/v) BSA and 0.5% Triton-X 100 supplemented with cOmplete™ Mini, EDTA-free protease inhibitor cocktail (Roche; 11836170001)].

Endocytosis assays using cell-surface biotinylation

All reactions were carried out on ice unless specified. Growth medium was aspirated from cells, which were then washed twice with ice-cold PBS. Cells were incubated for 1 h on ice with freshly prepared EZ-link™ Sulfo-NHS-SS-Biotin (Thermo Fisher Scientific; 0.25 mg ml^{-1}) before biotin was quenched by washing twice with PBS containing 100 mM glycine. Internalisation was allowed to proceed for various times by adding pre-warmed Upd2–GFP and incubating at 25°C. Cells were returned to ice and washed twice with PBS. Cell-surface biotin was cleaved by washing cells three times for 20 min with MESNa [100 mM 2-mercaptoethanesulfonate, added fresh for each incubation to 50 mM Tris-HCl pH8.6, 100 mM NaCl, 1 mM EDTA and 0.2% (w/v) BSA]. Cells were then washed three times in PBS. Reduced disulphide bonds were alkylated for 10 min with 500 mM iodoacetamide in PBS, before two final PBS washes. Cells were then lysed for 30 min and lysates were centrifuged at 18,000 ***g*** for 10 min. Streptavidin–agarose (15 µl) was washed three times with lysis buffer and incubated with cell lysate (10–30 µg) overnight at 4°C with rotation. Beads were then washed three times with lysis buffer and boiled for 5 min at 95°C in 20 µl Laemmli SDS–PAGE buffer, before SDS–PAGE and western blotting. Lysis buffer: 20 mM Tris-HCl pH7.5, 150 mM NaCl, 1 mM EDTA, 1 mM EGTA, 1% Triton X-100, 1 mM β-glycerophosphate, 25 mM Na-Pyrophosphate, 1 mM Na_3VO_4, 1 µg ml^{-1} microcystin and 25 mM N-ethylmaleimide supplemented with cOmplete™ Mini, EDTA-free protease inhibitor cocktail (Roche; 11836170001).

10×STAT–Luciferase detection

Cells were seeded in a 12-well plate at 5×10^5 cells per well 1 day prior to transfection. Cells were transfected with 0.5 µg *10×STAT–Luciferase* and 0.5 µg pAct-Renilla (pAc-Ren, internal control for transfection; Müller et al., 2005) for 1 day and then transferred to a 96-well plate at 5×10^4 cells per well. Cells were treated with conditioned medium containing Upd2–GFP for 18 h. Luciferase activity was measured using the Dual-Glo Luciferase Assay System (Promega), following the manufacturer's instructions, using a 1:5 dilution of DualGlo-luciferase in distilled water. The Dual-Glo Stop and Glo Luciferase Assay reagent (1:5 dilution) was added to the plate at an equal volume to the culture medium in the wells and incubated for at least 10 min. The firefly luciferase signal was measured using a Thermo Scientific Varioskan Flash Luminometer. An equal volume of Dual-Glo Stop and Glo reagent was then added and incubated for at least a further 10 min to allow measurement of the Renilla luciferase (RL) signal. Luciferase activity was calculated as firefly luciferase value normalised to the internal transfection control (RL).

Calf intestinal alkaline phosphatase treatment

STAT92E was immunoprecipitated from cells lysed in lysis buffer [PBS containing 1 mM $MgCl_2$, 0.1% (w/v) BSA, 0.5% Triton-X 100 supplemented with cOmplete™ Mini, EDTA-free protease inhibitor cocktail (Roche)]. Calf intestinal phosphatase (CIP; M0290S, NEB) was added at 1 unit per 1 µg protein then incubated for 1 h at 37°C. The reaction was stopped by addition of Laemmli SDS–PAGE buffer and boiling at 95°C for 5 min.

Quantitative PCR

RNA extraction was carried out using TRI reagent (Sigma-Aldrich; T9424) and reverse transcribed using the High Capacity RNA-to-cDNA™ kit (Applied Biosystems; 4387406). cDNA was diluted 1:10 and relative mRNA levels of *socs36E, Dome*, *lama*, *AP2*, *Hrs* and *TSG101* were quantified using qPCR. This was performed using SYBR Green JumpStart™ Taq ReadyMix™ (Sigma-Aldrich; S4438) and the primers listed in Table S2, on a Bio-Rad CFX96 real-time system, C100 Touch thermal cycler or Applied Biosystems QuantStudio 12K Flex. A standard curve of diluted template was used to interpolate the quantity of target gene in the test samples. Results for each target were normalised to levels of the reference gene, ribosomal protein L32 (Rpl32) mRNA, within each well.

Site-directed mutagenesis

Site-directed mutagenesis was carried out using a QuikChange Site-Directed Mutagenesis kit (Agilent Technologies), according to the manufacturer's instructions. Sequencing of plasmid DNA was carried out at the University of Sheffield's Core Genomic Facility, and results were analysed using ApE (ApE, A plasmid Editor v2.0.50; https://jorgensen.biology.utah.edu/wayned/ape/).

Mass spectrometry methods

STAT92E–GFP samples, prepared from GFP-trap beads or gel bands, were processed for mass spectrometry (MS) according to standard procedures. Samples were reduced with TCEP, followed by alkylation with iodoacetamide and digestion with trypsin or GluC. For some samples additional processing steps were required; for example, the use of HiPPR Detergent Removal spin columns (Thermo Fisher Scientific) for initial Triton removal or microscale solid phase extraction TiO_2 tips (Thermo Fisher Scientific) to enrich phosphorylated peptides. STAT92E–GFP peptides were analysed in an LTQ Orbitrap Elite (Thermo Fisher Scientific) hybrid ion trap-orbitrap mass spectrometer equipped with an EASY-Spray Ion Source hyphenated to a Dionex Ultimate 3000 uHPLC (Thermo Fisher Scientific). Peptides were trapped with an Acclaim™ PepMap™ 100 C18 trap column (3 µm particle size, 75 µm × 150 mm) and separated on an EASY-Spray™ C18 column (2 µm particle size, 50 µm × 150 mm) using an 80 min gradient with 0.1% formic acid in water (mobile phase A) and 0.1% formic acid in 80% acetonitrile (mobile phase B). Positive MS survey scans were acquired in the FT-orbitrap analyzer using an *m*/*z* window from 375 to 1600, and a resolution of 60,000. The 20 most intense precursor ions were selected for the acquisition of MS/MS spectra in the ion trap (Normal Scan Rate) using collision-induced dissociation (CID) with normalized collision energy of 35% and isolation width of 2 Th. Raw MS/MS data files were used for protein identification using MaxQuant software (Cox and Mann, 2008) with default parameters, except for the following: protein database was the *Drosophila melanogaster* Uniprot proteome (downloaded on 25 August 2016) and a FASTA file containing the theoretical sequence of STAT92E–GFP and STAT92E^{T702V}–GFP; LFQ quantification and iBAQ values were selected for calculation; variable modifications, oxidation (M) and phosphorylation (STY); fixed modifications, carbamydomethylation (C). Relevant spectra were manually inspected after annotation with pLabel software (Li et al., 2005; Wang et al., 2007). A detailed description of mass spectrometry methods (sample preparation, mass spectrometry analysis and data processing), together with mass spectrometry data and annotated relevant spectra (phosphorylated Y704, T47, S227 and T702), has been deposited at the ProteomeXchange Consortium via the PRIDE partner repository (Deutsch et al., 2020). The identifier number of the dataset is PXD020719.

Immunofluorescence detection of nuclear and cytoplasmic STAT92E–GFP

Following dsRNA treatment or transfection with STAT92E constructs, cells were plated on sterile coverslips, pretreated overnight with 0.1 mg/ml poly-L-lysine. Following treatment with Upd2–GFP, cells were fixed in 4% paraformaldehyde for 20 minutes, then quenched with two 5-minute washes with 50 mM ammonium chloride in PBS. Following permeabilisation with 0.2% Triton X-100 in PBS for 5 minutes, coverslips were washed three times with PBS and incubated with 0.2% fish skin gelatin (FSG) for 1 h at room temperature. Following three washes with PBS, coverslips were incubated with anti-GFP antibody (Abnova, PAB10341; diluted 1:2000 in PBS containing 0.2% FSG) and then incubated with secondary antibody for 45 minutes in the dark. To stain cell nuclei, a final concentration of 1 µg/ml DAPI was added for 5 minutes. Coverslips were then washed three times in 0.2% FSG in PBS, before mounting onto slides with ProLong™ Gold Antifade mountant (Thermo Fisher Scientific, P10144). A DeltaVision/GE Healthcare OMX optical microscope (version 4) with oil-immersion objective (60× NA 1.42, PlanApochromat Olympus) was used for wide-field and SIM immunofluorescence image acquisition. Deconvolution and image registration (for alignment of SIM images) was carried out using the DeltaVision OMX softWoRx 6.0 software. Analysis of microscopy images was carried out using ImageJ (NIH, Bethesda, MD, USA). Four regions of interest (ROI) of equal size were drawn within each transfected cell: two within the nucleus and two within the cytoplasm. Intensity measures were averaged for the nucleus and divided by the average intensity for the cytoplasm.

Acknowledgements

We acknowledge Addgene for the STAT92E–GFP and pAc-sgRNA-Cas9 constructs. Images were collected in the Wolfson Light Microscopy Facility using a Nikon wide-field camera, funded by MRC Shima award (MR/K015753/1). Mass spectrometry was performed in the University of Sheffield, Faculty of Science biOMICs Facility.

Competing interests

The authors declare no competing or financial interests.

Author contributions

Conceptualization: R.M., K.V., E.S.; Methodology: R.M., K.V., A.E.A.-M., P.S., M.Z., E.S.; Investigation: R.M., K.V., A.E.A.-M., P.S.; Data curation: R.M., K.V., E.S.; Writing - original draft: R.M., A.E.A.-M., E.S.; Writing - review & editing: R.M., K.V., A.E.A.-M., P.S., M.Z., E.S.; Supervision: M.Z., E.S.; Project administration: E.S.; Funding acquisition: E.S.

Funding

R.M. was funded by a University of Sheffield Centre for Membrane Interactions and Dynamics PhD studentship; K.V. by a Cancer Research UK studentship (C12332/A10681); P.S. by a Biotechnology and Biological Sciences Research Council CASE award (BB/M011151/1).

Data availability

Mass spectrometry methods and data have been deposited at the ProteomeXchange Consortium via the PRIDE partner repository http://www.ebi.ac.uk/pride. The identification number of the dataset is PXD020719.

Supplementary information

Supplementary information available online at https://jcs.biologists.org/lookup/doi/10.1242/jcs.246199.supplemental

Peer review history

The peer review history is available online at https://jcs.biologists.org/lookup/doi/10.1242/jcs.246199.reviewer-comments.pdf

References

Baeg, G.-H., Zhou, R. and Perrimon, N. (2005). Genome-wide RNAi analysis of JAK/STAT signaling components in Drosophila. *Genes Dev.* **19**, 1861-1870. doi:10.1101/gad.1320705

Bassett, A. R., Tibbit, C., Ponting, C. P. and Liu, J.-L. (2014). Mutagenesis and homologous recombination in Drosophila cell lines using CRISPR/Cas9. *Biol. Open* **3**, 42-49. doi:10.1242/bio.20137120

Begitt, A., Meyer, T., van Rossum, M. and Vinkemeier, U. (2000). Nucleocytoplasmic translocation of Stat1 is regulated by a leucine-rich export signal in the coiled-coil domain. *Proc. Natl. Acad. Sci. USA* **97**, 10418-10423. doi:10.1073/pnas.190318397

Brown, S. and Zeidler, M. P. (2008). Unphosphorylated STATs go nuclear. *Curr. Opin. Genet. Dev.* **18**, 455-460. doi:10.1016/j.gde.2008.09.002

Brown, S., Hu, N. and Hombria, J. C.-G. (2001). Identification of the first invertebrate interleukin JAK/STAT receptor, the Drosophila gene domeless. *Curr. Biol.* **11**, 1700-1705. doi:10.1016/S0960-9822(01)00524-3

Carroll, B. and Dunlop, E. A. (2017). The lysosome: a crucial hub for AMPK and mTORC1 signalling. *Biochem. J.* **474**, 1453-1466. doi:10.1042/BCJ20160780

Cendrowski, J., Mamińska, A. and Miaczynska, M. (2016). Endocytic regulation of cytokine receptor signaling. *Cytokine Growth Factor. Rev.* **32**, 63-73. doi:10.1016/j.cytogfr.2016.07.002

Chanut-Delalande, H., Jung, A. C., Baer, M. M., Lin, L., Payre, F. and Affolter, M. (2010). The Hrs/Stam complex acts as a positive and negative regulator of RTK signaling during Drosophila development. *PLoS ONE* **5**, e10245. doi:10.1371/journal.pone.0010245

Chen, X., Vinkemeier, U., Zhao, Y., Jeruzalmi, D., Darnell, J. E., Jr and Kuriyan, J. (1998). Crystal structure of a tyrosine phosphorylated STAT-1 dimer bound to DNA. *Cell* **93**, 827-839. doi:10.1016/S0092-8674(00)81443-9

Cherbas, L., Willingham, A., Zhang, D., Yang, L., Zou, Y., Eads, B. D., Carlson, J. W., Landolin, J. M., Kapranov, P., Dumais, J. et al. (2011). The transcriptional diversity of 25 Drosophila cell lines. *Genome Res.* **21**, 301-314. doi:10.1101/gr.112961.110

Chmiest, D., Sharma, N., Zanin, N., Viaris de Lesegno, C., Shafaq-Zadah, M., Sibut, V., Dingli, F., Hupé, P., Wilmes, S., Piehler, J. et al. (2016).

Spatiotemporal control of interferon-induced JAK/STAT signalling and gene transcription by the retromer complex. *Nat. Commun.* **7**, 13476. doi:10.1038/ncomms13476

Chung, J., Uchida, E., Grammer, T. C. and Blenis, J. (1997). STAT3 serine phosphorylation by ERK-dependent and -independent pathways negatively modulates its tyrosine phosphorylation. *Mol. Cell. Biol.* **17**, 6508-6516. doi:10.1128/MCB.17.11.6508

Costa-Pereira, A. P., Bonito, N. A. and Seckl, M. J. (2011). Dysregulation of janus kinases and signal transducers and activators of transcription in cancer. *Am. J. Cancer Res.* **1**, 806-816.

Cox, J. and Mann, M. (2008). MaxQuant enables high peptide identification rates, individualized p.p.b.-range mass accuracies and proteome-wide protein quantification. *Nat. Biotechnol.* **26**, 1367-1372. doi:10.1038/nbt.1511

Deutsch, E. W., Bandeira, N., Sharma, V., Perez-Riverol, Y., Carver, J. J., Kundu, D. J., García-Seisdedos, D., Jarnuczak, A. F., Hewapathirana, S., Pullman, B. S. et al. (2020). The ProteomeXchange consortium in 2020: enabling 'big data' approaches in proteomics. *Nucleic Acids Res.* **48**, D1145-D1152. doi:10.1093/nar/gkz984

Devergne, O., Ghiglione, C. and Noselli, S. (2007). The endocytic control of JAK/STAT signalling in Drosophila. *J. Cell Sci.* **120**, 3457-3464. doi:10.1242/jcs.005926

Di Guglielmo, G. M., Le Roy, C., Goodfellow, A. F. and Wrana, J. L. (2003). Distinct endocytic pathways regulate TGF-β receptor signalling and turnover. *Nat. Cell Biol.* **5**, 410-421. doi:10.1038/ncb975

Dittrich, E., Haft, C. R., Muys, L., Heinrich, P. C. and Graeve, L. (1996). A di-leucine motif and an upstream serine in the interleukin-6 (IL-6) signal transducer gp130 mediate ligand-induced endocytosis and down-regulation of the IL-6 receptor. *J. Biol. Chem.* **271**, 5487-5494. doi:10.1074/jbc.271.10.5487

Doray, B., Lee, I., Knisely, J., Bu, G. and Kornfeld, S. (2007). The γ/σ1 and α/σ2 hemicomplexes of clathrin adaptors AP-1 and AP-2 harbor the dileucine recognition site. *Mol. Biol. Cell* **18**, 1887-1896. doi:10.1091/mbc.e07-01-0012

Ekas, L. A., Cardozo, T. J., Flaherty, M. S., McMillan, E. A., Gonsalves, F. C. and Bach, E. A. (2010). Characterization of a dominant-active STAT that promotes tumorigenesis in Drosophila. *Dev. Biol.* **344**, 621-636. doi:10.1016/j.ydbio.2010.05.497

Fisher, K. H., Stec, W., Brown, S. and Zeidler, M. P. (2016). Mechanisms of JAK/STAT pathway negative regulation by the short coreceptor Eye Transformer/Latran. *Mol. Biol. Cell* **27**, 434-441. doi:10.1091/mbc.e15-07-0546

Flaherty, M. S., Zavadil, J., Ekas, L. A. and Bach, E. A. (2009). Genome-wide expression profiling in the Drosophila eye reveals unexpected repression of notch signaling by the JAK/STAT pathway. *Dev. Dyn.* **238**, 2235-2253. doi:10.1002/dvdy.21989

German, C. L., Sauer, B. M. and Howe, C. L. (2011). The STAT3 beacon: IL-6 recurrently activates STAT 3 from endosomal structures. *Exp. Cell Res.* **317**, 1955-1969. doi:10.1016/j.yexcr.2011.05.009

Grönholm, J., Ungureanu, D., Vanhatupa, S., Rämet, M. and Silvennoinen, O. (2010). Sumoylation of Drosophila transcription factor STAT92E. *J. Innate Immun.* **2**, 618-624. doi:10.1159/000318676

Guschin, D. Y., Waite, A. J., Katibah, G. E., Miller, J. C., Holmes, M. C. and Rebar, E. J. (2010). A rapid and general assay for monitoring endogenous gene modification. *Methods Mol. Biol.* **649**, 247-256. doi:10.1007/978-1-60761-753-2_15

Henne, W. M., Stenmark, H. and Emr, S. D. (2013). Molecular mechanisms of the membrane sculpting ESCRT pathway. *Cold Spring Harb. Perspect. Biol.* **5**, a016766. doi:10.1101/cshperspect.a016766

Horn, T., Sandmann, T. and Boutros, M. (2010). Design and evaluation of genome-wide libraries for RNA interference screens. *Genome Biol.* **11**, R61. doi:10.1186/gb-2010-11-6-r61

Hou, X. S., Melnick, M. B. and Perrimon, N. (1996). Marelle acts downstream of the Drosophila HOP/JAK kinase and encodes a protein similar to the mammalian STATs. *Cell* **84**, 411-419. doi:10.1016/S0092-8674(00)81286-6

Karsten, P., Häder, S. and Zeidler, M. P. (2002). Cloning and expression of Drosophila SOCS36E and its potential regulation by the JAK/STAT pathway. *Mech. Dev.* **117**, 343-346. doi:10.1016/S0925-4773(02)00216-2

Karsten, P., Plischke, I., Perrimon, N. and Zeidler, M. P. (2006). Mutational analysis reveals separable DNA binding and trans-activation of Drosophila STAT92E. *Cell. Signal.* **18**, 819-829. doi:10.1016/j.cellsig.2005.07.006

Kelly, B. T., McCoy, A. J., Späte, K., Miller, S. E., Evans, P. R., Höning, S. and Owen, D. J. (2008). A structural explanation for the binding of endocytic dileucine motifs by the AP2 complex. *Nature* **456**, 976-979. doi:10.1038/nature07422

Kermorgant, S. and Parker, P. J. (2008). Receptor trafficking controls weak signal delivery: a strategy used by c-Met for STAT3 nuclear accumulation. *J. Cell Biol.* **182**, 855-863. doi:10.1083/jcb.200806076

Lawrence, R. E., Fromm, S. A., Fu, Y., Yokom, A. L., Kim, D. J., Thelen, A. M., Young, L. N., Lim, C.-Y., Samelson, A. J., Hurley, J. H. et al. (2019). Structural mechanism of a Rag GTPase activation checkpoint by the lysosomal folliculin complex. *Science* **366**, 971-977. doi:10.1126/science.aax0364

Li, D., Fu, Y., Sun, R., Ling, C. X., Wei, Y., Zhou, H., Zeng, R., Yang, Q., He, S. and Gao, W. (2005). pFind: a novel database-searching software system for automated peptide and protein identification via tandem mass spectrometry. *Bioinformatics* **21**, 3049-3050. doi:10.1093/bioinformatics/bti439

Makki, R., Meister, M., Pennetier, D., Ubeda, J.-M., Braun, A., Daburon, V., Krzemień, J., Bourbon, H.-M., Zhou, R., Vincent, A. et al. (2010). A short receptor downregulates JAK/STAT signalling to control the Drosophila cellular immune response. *PLoS Biol.* **8**, e1000441. doi:10.1371/journal.pbio.1000441

Mao, X., Ren, Z., Parker, G. N., Sondermann, H., Pastorello, M. A., Wang, W., McMurray, J. S., Demeler, B., Darnell, J. E., Jr and Chen, X. (2005). Structural bases of unphosphorylated STAT1 association and receptor binding. *Mol. Cell* **17**, 761-771. doi:10.1016/j.molcel.2005.02.021

Marchetti, M., Monier, M.-N., Fradagrada, A., Mitchell, K., Baychelier, F., Eid, P., Johannes, L. and Lamaze, C. (2006). Stat-mediated signaling induced by type I and type II interferons (IFNs) is differentially controlled through lipid microdomain association and clathrin-dependent endocytosis of IFN receptors. *Mol. Biol. Cell* **17**, 2896-2909. doi:10.1091/mbc.e06-01-0076

Mayor, S., Parton, R. G. and Donaldson, J. G. (2014). Clathrin-independent pathways of endocytosis. *Cold Spring Harbor Perspect. Biol.* **6**, a016758. doi:10.1101/cshperspect.a016758

McBride, K. M., McDonald, C. and Reich, N. C. (2000). Nuclear export signal located within theDNA-binding domain of the STAT1transcription factor. *EMBO J.* **19**, 6196-6206. doi:10.1093/emboj/19.22.6196

Mettlen, M., Chen, P.-H., Srinivasan, S., Danuser, G. and Schmid, S. L. (2018). Regulation of clathrin-mediated endocytosis. *Annu. Rev. Biochem.* **87**, 871-896. doi:10.1146/annurev-biochem-062917-012644

Moore, R., Pujol, M. G., Zhu, Z. and Smythe, E. (2018). Interplay of endocytosis and growth factor receptor signalling. *Prog. Mol. Subcell. Biol.* **57**, 181-202. doi:10.1007/978-3-319-96704-2_7

Müller, P., Boutros, M. and Zeidler, M. P. (2008). Identification of JAK/STAT pathway regulators—insights from RNAi screens. *Semin. Cell Dev. Biol.* **19**, 360-369. doi:10.1016/j.semcdb.2008.06.001

Müller, P., Kuttenkeuler, D., Gesellchen, V., Zeidler, M. P. and Boutros, M. (2005). Identification of JAK/STAT signalling components by genome-wide RNAi interference. *Nature* **436**, 871-875. doi:10.1038/nature03869

O'Shea, J. J., Schwartz, D. M., Villarino, A. V., Gadina, M., McInnes, I. B. and Laurence, A. (2015). The JAK-STAT pathway: impact on human disease and therapeutic intervention. *Annu. Rev. Med.* **66**, 311-328. doi:10.1146/annurev-med-051113-024537

Owen, D. J., Collins, B. M. and Evans, P. R. (2004). Adaptors for clathrin coats: structure and function. *Annu. Rev. Cell Dev. Biol.* **20**, 153-191. doi:10.1146/annurev.cellbio.20.010403.104543

Pandey, A., Fernandez, M. M., Steen, H., Blagoev, B., Nielsen, M. M., Roche, S., Mann, M. and Lodish, H. F. (2000). Identification of a novel immunoreceptor tyrosine-based activation motif-containing molecule, STAM2, by mass spectrometry and its involvement in growth factor and cytokine receptor signaling pathways. *J. Biol. Chem.* **275**, 38633-38639. doi:10.1074/jbc.M007849200

Ren, W., Zhang, Y., Li, M., Wu, L., Wang, G., Baeg, G.-H., You, J., Li, Z. and Lin, X. (2015). Windpipe controls Drosophila intestinal homeostasis by regulating JAK/STAT pathway via promoting receptor endocytosis and lysosomal degradation. *PLoS Genet.* **11**, e1005180. doi:10.1371/journal.pgen.1005180

Robinson, M. S. (2004). Adaptable adaptors for coated vesicles. *Trends Cell Biol.* **14**, 167-174. doi:10.1016/j.tcb.2004.02.002

Schindler, C., Shuai, K., Prezioso, V. R. and Darnell, J. E.Jr. (1992). Interferon-dependent tyrosine phosphorylation of a latent cytoplasmic transcription factor. *Science* **257**, 809-813. doi:10.1126/science.1496401

Seibel, N. M., Eljouni, J., Nalaskowski, M. M. and Hampe, W. (2007). Nuclear localization of enhanced green fluorescent protein homomultimers. *Anal. Biochem.* **368**, 95-99. doi:10.1016/j.ab.2007.05.025

Shi, S., Larson, K., Guo, D., Lim, S. J., Dutta, P., Yan, S.-J. and Li, W. X. (2008). Drosophila STAT is required for directly maintaining HP1 localization and heterochromatin stability. *Nat. Cell Biol.* **10**, 489-496. doi:10.1038/ncb1713

Shimizu, H., Woodcock, S. A., Wilkin, M. B., Trubenová, B., Monk, N. A. M. and Baron, M. (2014). Compensatory flux changes within an endocytic trafficking network maintain thermal robustness of Notch signaling. *Cell* **157**, 1160-1174. doi:10.1016/j.cell.2014.03.050

Sigismund, S. and Scita, G. (2018). The 'endocytic matrix reloaded' and its impact on the plasticity of migratory strategies. *Curr. Opin. Cell Biol.* **54**, 9-17. doi:10.1016/j.ceb.2018.02.006

Sigismund, S., Woelk, T., Puri, C., Maspero, E., Tacchetti, C., Transidico, P., Di Fiore, P. P. and Polo, S. (2005). Clathrin-independent endocytosis of ubiquitinated cargos. *Proc. Natl. Acad. Sci. USA* **102**, 2760-2765. doi:10.1073/pnas.0409817102

Sigismund, S., Algisi, V., Nappo, G., Conte, A., Pascolutti, R., Cuomo, A., Bonaldi, T., Argenzio, E., Verhoef, L. G. G. C., Maspero, E. et al. (2013). Threshold-controlled ubiquitination of the EGFR directs receptor fate. *EMBO J.* **32**, 2140-2157. doi:10.1038/emboj.2013.149

Silver, D. L., Geisbrecht, E. R. and Montell, D. J. (2005). Requirement for JAK/STAT signaling throughout border cell migration in Drosophila. *Development* **132**, 3483-3492. doi:10.1242/dev.01910

Sousa, L. P., Lax, I., Shen, H., Ferguson, S. M., De Camilli, P. and Schlessinger, J. (2012). Suppression of EGFR endocytosis by dynamin depletion reveals that EGFR signaling occurs primarily at the plasma membrane. *Proc. Natl. Acad. Sci. USA* **109**, 4419-4424. doi:10.1073/pnas.1200164109

Stahl, N. and Yancopoulos, G. D. (1994). The tripartite CNTF receptor complex: activation and signaling involves components shared with other cytokines. *J. Neurobiol.* **25**, 1454-1466. doi:10.1002/neu.480251111

Stark, G. R. and Darnell, J. E.Jr. (2012). The JAK-STAT pathway at twenty. *Immunity* **36**, 503-514. doi:10.1016/j.immuni.2012.03.013

Stec, W., Vidal, O. and Zeidler, M. P. (2013). Drosophila SOCS36E negatively regulates JAK/STAT pathway signaling via two separable mechanisms. *Mol. Biol. Cell* **24**, 3000-3009. doi:10.1091/mbc.e13-05-0275

Takeshita, T., Arita, T., Higuchi, M., Asao, H., Endo, K., Kuroda, H., Tanaka, N., Murata, K., Ishii, N. and Sugamura, K. (1997). STAM, signal transducing adaptor molecule, is associated with Janus kinases and involved in signaling for cell growth and c-myc induction. *Immunity* **6**, 449-457. doi:10.1016/S1074-7613(00)80288-5

Teis, D., Wunderlich, W. and Huber, L. A. (2002). Localization of the MP1-MAPK scaffold complex to endosomes is mediated by p14 and required for signal transduction. *Dev. Cell* **3**, 803-814. doi:10.1016/S1534-5807(02)00364-7

Thiel, S., Dahmen, H., Martens, A., Müller-Newen, G., Schaper, F., Heinrich, P. C. and Graeve, L. (1998). Constitutive internalization and association with adaptor protein-2 of the interleukin-6 signal transducer gp130. *FEBS Lett.* **441**, 231-234. doi:10.1016/S0014-5793(98)01559-2

Tognon, E., Wollscheid, N., Cortese, K., Tacchetti, C. and Vaccari, T. (2014). ESCRT-0 is not required for ectopic Notch activation and tumor suppression in Drosophila. *PLoS ONE* **9**, e93987. doi:10.1371/journal.pone.0093987

Traub, L. M. (2003). Sorting it out: AP-2 and alternate clathrin adaptors in endocytic cargo selection. *J. Cell Biol.* **163**, 203-208. doi:10.1083/jcb.200309175

Vander Ark, A., Cao, J. and Li, X. (2018). TGF-β receptors: in and beyond TGF-β signaling. *Cell. Signal.* **52**, 112-120. doi:10.1016/j.cellsig.2018.09.002

Vidal, O. M., Stec, W., Bausek, N., Smythe, E. and Zeidler, M. P. (2010). Negative regulation of Drosophila JAK-STAT signalling by endocytic trafficking. *J. Cell Sci.* **123**, 3457-3466. doi:10.1242/jcs.066902

Vieira, A. V., Lamaze, C. and Schmid, S. L. (1996). Control of egf receptor signaling by clathrin-mediated endocytosis. *Science* **274**, 2086-2089. doi:10.1126/science.274.5295.2086

Vietri, M., Radulovic, M. and Stenmark, H. (2019). The many functions of ESCRTs. *Nat. Rev. Mol. Cell Biol.*. **21**, 25-42. doi:10.1038/s41580-019-0177-4

Villarino, A. V., Kanno, Y. and O'Shea, J. J. (2017). Mechanisms and consequences of Jak-STAT signaling in the immune system. *Nat. Immunol.* **18**, 374-384. doi:10.1038/ni.3691

Villaseñor, R., Nonaka, H., Del Conte-Zerial, P., Kalaidzidis, Y. and Zerial, M. (2015). Regulation of EGFR signal transduction by analogue-to-digital conversion in endosomes. *eLife* **4**, e06156. doi:10.7554/eLife.06156

Villaseñor, R., Kalaidzidis, Y. and Zerial, M. (2016). Signal processing by the endosomal system. *Curr. Opin. Cell Biol.* **39**, 53-60. doi:10.1016/j.ceb.2016.02.002

Wang, L. H., Li, D. Q., Fu, Y., Wang, H. P., Zhang, J. F., Yuan, Z. F., Sun, R. X., Zeng, R., He, S. M. and Gao, W. (2007). pFind 2.0: a software package for peptide and protein identification via tandem mass spectrometry. *Rapid Commun. Mass Spectrom.* **21**, 2985-2991. doi:10.1002/rcm.3173

Wang, R., Cherukuri, P. and Luo, J. (2005). Activation of Stat3 sequence-specific DNA binding and transcription by p300/CREB-binding protein-mediated acetylation. *J. Biol. Chem.* **280**, 11528-11534. doi:10.1074/jbc.M413930200

Waterhouse, A., Bertoni, M., Bienert, S., Studer, G., Tauriello, G., Gumienny, R., Heer, F. T., de Beer, T. A. P., Rempfer, C., Bordoli, L. et al. (2018). SWISS-MODEL: homology modelling of protein structures and complexes. *Nucleic Acids Res.* **46**, W296-W303. doi:10.1093/nar/gky427

Weinberg, Z. Y. and Puthenveedu, M. A. (2019). Regulation of G protein-coupled receptor signaling by plasma membrane organization and endocytosis. *Traffic* **20**, 121-129. doi:10.1111/tra.12628

Wenta, N., Strauss, H., Meyer, S. and Vinkemeier, U. (2008). Tyrosine phosphorylation regulates the partitioning of STAT1 between different dimer conformations. *Proc. Natl. Acad. Sci. USA* **105**, 9238-9243. doi:10.1073/pnas.0802130105

Wright, V. M., Vogt, K. L., Smythe, E. and Zeidler, M. P. (2011). Differential activities of the Drosophila JAK/STAT pathway ligands Upd, Upd2 and Upd3. *Cell. Signal.* **23**, 920-927. doi:10.1016/j.cellsig.2011.01.020

Yan, R., Small, S., Desplan, C., Dearolf, C. R. and Darnell, J. E.Jr. (1996). Identification of a Stat gene that functions in Drosophila development. *Cell* **84**, 421-430. doi:10.1016/S0092-8674(00)81287-8

Zeidler, M. P. and Bausek, N. (2013). The Drosophila JAK-STAT pathway. *JAKSTAT* **2**, e25353. doi:10.4161/jkst.25353

Supplementary Figures

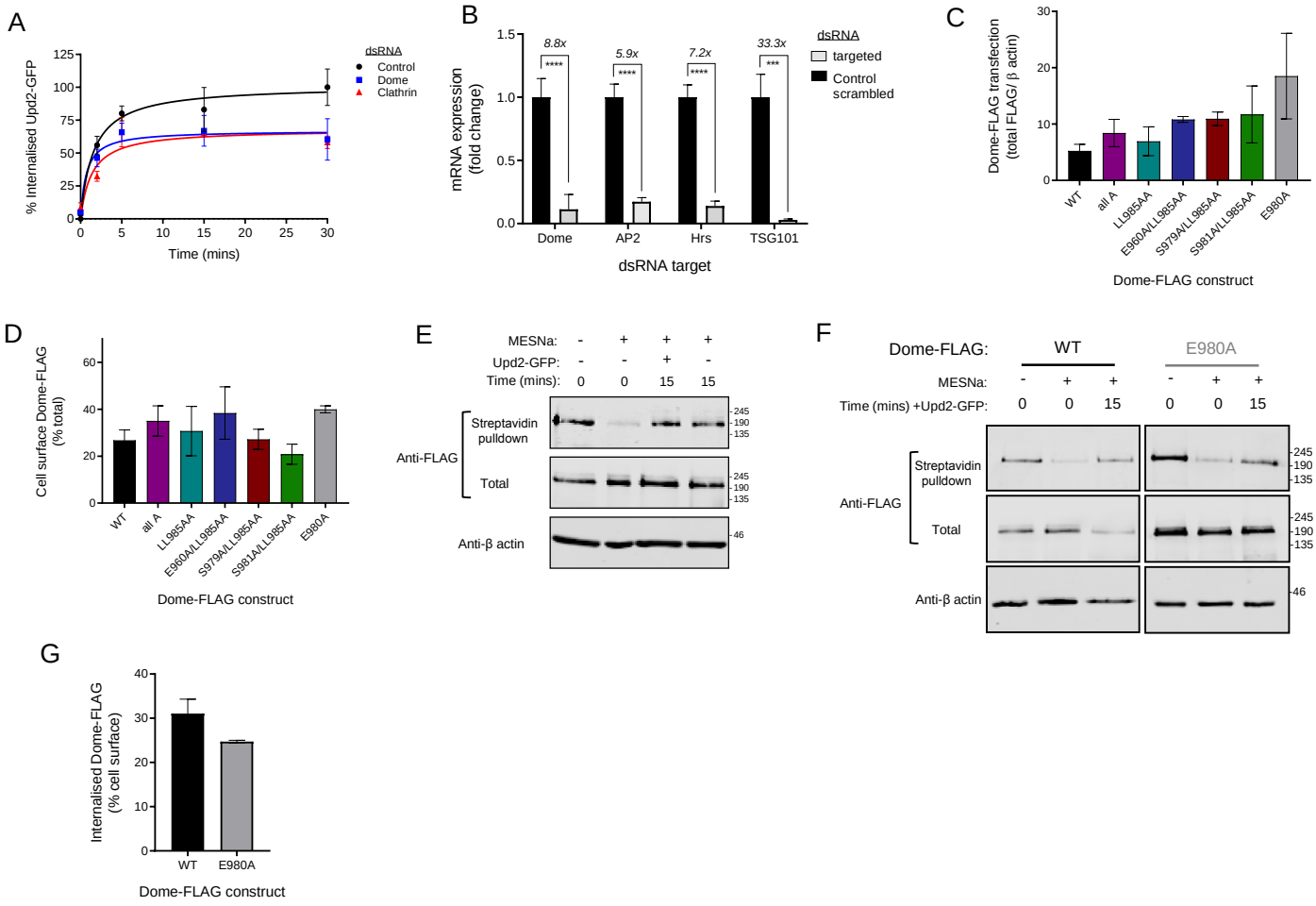

Figure S1

(A) CME is the route of GFP-Upd2 uptake at low ligand concentrations. S2R+ cells were treated for 5 days with control, clathrin (CHC) or Dome dsRNA. Cells were incubated with 3 nM Upd2-GFP for indicated time points at 25°C. Following acid washes, cell lysates were analysed with an anti-GFP ELISA. Internalised Upd2-GFP is expressed as percentage of the total amount internalised at 30 minutes. Graph is a representative experiment where each point is mean of triplicates +/- s.d. **(B)** mRNA levels of dsRNA targets following knockdown. S2R+ cells were treated with dsRNA 5 days prior to TRIzol RNA extraction. mRNA levels were analysed using qPCR, with levels of target mRNA normalised to rpl32 mRNA. Ratios are plotted as fold change compared to control dsRNA for each target mRNA. Graph represents the mean of triplicates +/- s.d. for at least 2 independent experiments (Dome = 2 repeats), or mean +/- s.e.m. for at least three independent experiments (AP2, Hrs and TSG101). Parametric, unpaired student's t-test was performed to compare control knockdown with targeted dsRNA knockdown, with ***p≤0.001, ****p≤0.0001. **(C)** Lysates from S2R+ cells transfected with FLAG-tagged Dome wild-type and mutants were prepared and subjected to SDS-PAGE and Western blotting with antibodies to FLAG and b-actin. The ratio of transfected Dome-FLAG construct is expressed as a function of the amount of b-actin. Graph is the mean ± s.d. of at least 2 independent experiments. Using student's t-test, there was no statistical difference between wild-type and mutant constructs. **(D)** Percentage of biotinylated Dome-FLAG at cell surface compared to total levels of transfected Dome-FLAG in cells expressing wild-type or mutant Dome-FLAG constructs. Using student's t-test, there was no statistical difference between wild-type and mutant constructs. **(E)** Dome is internalised efficiently in the absence of ligand. Sample immunoblot of cells transfected with Dome^{WT}-FLAG for 48hrs prior to cell surface biotinylation and endocytosis for 15 minutes +/- Upd2-GFP, followed by treatment +/- MESNa. Western blots were probed with antibodies as indicated. **(F)** Sample immunoblot of lysates from cells transfected with Dome^{WT}-FLAG or Dome^{E980A}-FLAG for 48 hrs prior to cell surface biotinylation and incubation at 25°C for times indicated +/- Upd2-GFP followed by treatment +/- MESNa. Western blots were probed with antibodies as indicated. **(G)** Quantitation of internalisation of Dome^{WT}-FLAG and Dome^{E980A}-FLAG. Percentage of cell-surface receptor that is internalised after 15 mins at 25°C. Background of biotinylated cell surface Dome-FLAG after 0 mins endocytosis and MESNa treatment was subtracted and internalised Dome-FLAG was then calculated as a percentage of total cell surface Dome-FLAG prior to MESNa treatment. Graphs represent mean +/- s.d. for 2 independent experiments and no significant differences were observed.

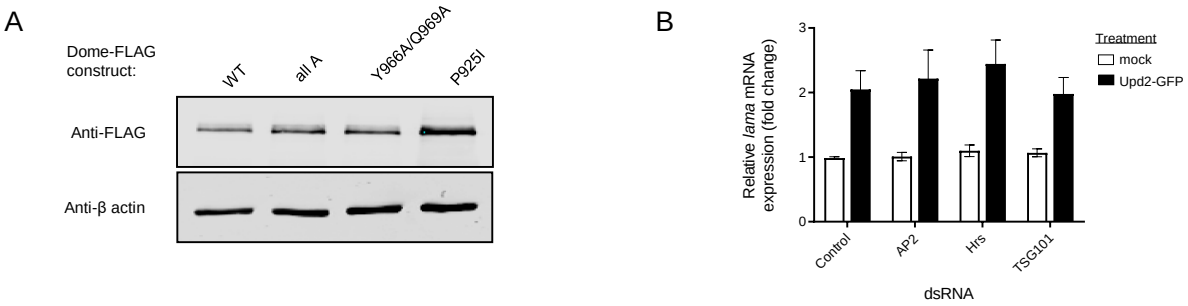

Figure S2:
(A) Sample immunoblot of relative transfection efficiencies of Dome^{WT}-FLAG, Dome^{allA}-FLAG, Dome$^{Y966A/Q969A}$-FLAG and Dome ^{P925I}-FLAG. Blots were probed with antibodies as indicated.
(B) *lama* expression is independent of endocytosis. S2R+ cells were treated with dsRNA against AP2, Hrs and TSG101 as well as non-targeting (control) dsRNA for 5 days. Cells were incubated with 3 nM Upd2-GFP for 2.5 hrs prior to RNA extraction. *lama* mRNA levels were normalised to that of reference gene Rpl32, and presented as fold change compared to mock-treated control samples. Results are expressed as means of triplicates +/- s.e.m. for 3 independent experiments.

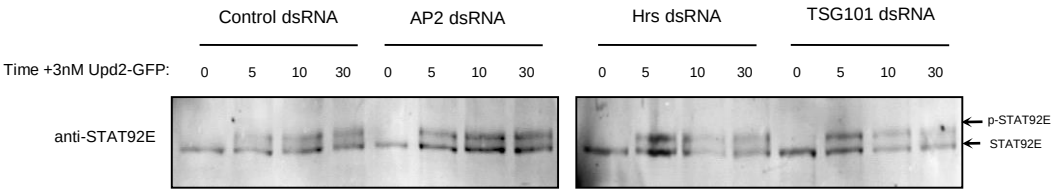

Figure S3: STAT92E phosphorylation is not regulated by endocytosis.
Representative immunoblot of control vs AP2, Hrs and TSG101 knockdown S2R+ cells treated with 3 nM Upd2-GFP at 25° C for the indicated times. Cells were treated with targeting dsRNA and incubated for 5 days at 25° C. Total protein extract was analysed by SDS-PAGE and immunoblotted with anti-STAT92E antibodies.

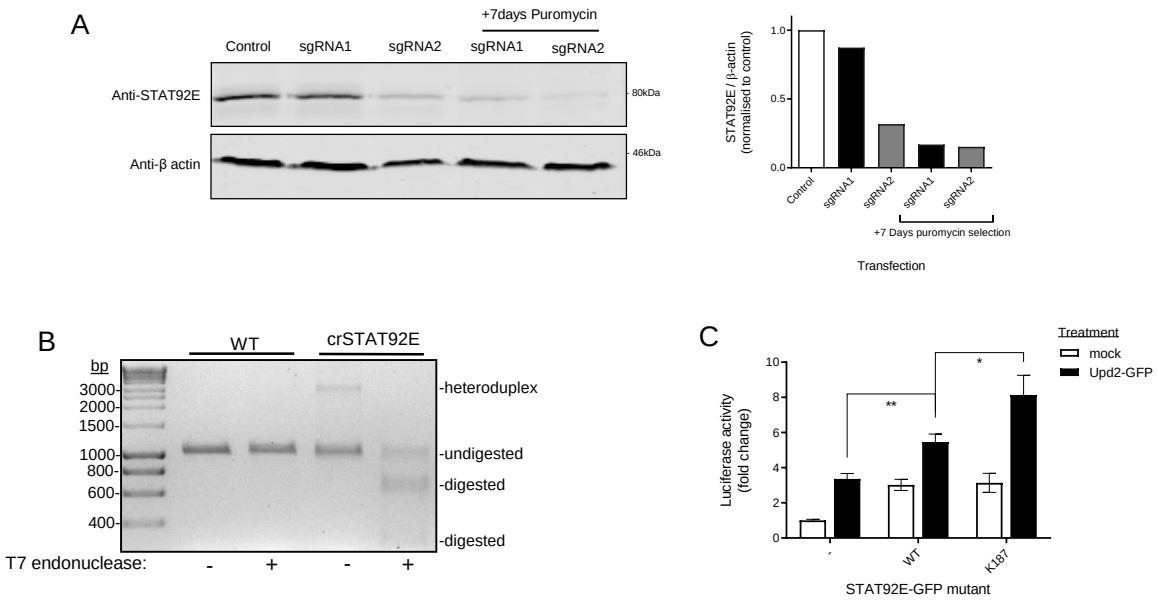

Figure S4: Generation and characterization of STAT92E negative S2R+ cells.
(A) Immunoblot and quantification demonstrating levels of STAT92E protein in cells transfected with pAc-sgRNA-Cas9 targeting STAT92E for 3 days, and then either with or without puromycin selection as indicated. Blots were probed with antibodies as indicated.
(B) T7-endonuclease assay demonstrates Cas9 induced mutation in the STAT92E gene. Genomic DNA was extracted from WT and crSTAT2 cell lines, and a 989bp region around the sgRNA target site was amplified by PCR. Addition of T7 endonuclease to the PCR product causes multiple bands for crSTAT2 cell line but not WT cells.
(C) Mutation of Lys187 increases STAT92E signalling. crSTAT cells were transfected with pAc-Ren, *10xSTAT-Luciferase* and pAc5.1 (-), $STAT92E^{WT}$-GFP or $STAT92E^{K187R}$-GFP. Cells were stimulated with 0.75 nM Upd2-GFP for 30 mins, then incubated in fresh media for 18 hrs followed by measurement of bioluminescence. Data is mean +/- s.e.m. from 3 independent experiments and normalised to cells transfected with pAc5.1 (-) and treated with 0 nM Upd2-GFP. *: $p<0.05$; **: $p<0.01$.

Table S1: SgRNA oligos

Oligo	Sequence
sgRNA1.1	TTCGACAACACGCCCATGGTTACC
sgRNA1.2	AACGGTAACCATGGGCGTGTTGTC
sgRNA2.1	TTCGACCATGTACCCGGTAACCAT
sgRNA2.2	AACATGGTTACCGGGTACATGGTC

Table S2: Primers for qPCR

Gene	CG number	Forward primer	Reverse primer
Rpl32	CG7939	GACGCTTCAAGGGACAGTATCTG	AAACGCGGTTCTGCATGAG
domeless	CG14226	ACTTTCGGTACTCCATCAGC	TGGACTCCACCTTGATGAG
tsg101	CG9712	GAGGAGACACAAATAACAAAGTACC	TGAGTGTCCATCAACCAAATAC
clathrin heavy chain(CHC)	CG9012	GTAGTAAAGATGACGCAACCAC	GTTCATGTCAATGATGACCACT
α-adaptin	CG4260	ACCAGCGAAAATTAACAAGC	GAGACGACTTCACACCCTTC
socs36A	CG15154	AGTGCTTTACTGCTGCGACT	TCGTCGAGTATTGCGAAGT
lama	CG10645	TGATATTGCTGCTTTCCTGGAC	TGGTTTGGCGATGGTTTTAT